Developing Continuous Predictive Controls for Ankle Angle and Moment Across Multiple Mobility Tasks

John Eganhouse
Marquette University

DEVELOPING CONTINUOUS PREDICTIVE CONTROLS FOR ANKLE ANGLE AND MOMENT ACROSS MULTIPLE MOBILITY TASKS

by

John Eganhouse

A Thesis submitted to the Faculty of the Graduate School,
Marquette University,
in Partial Fulfillment of the Requirements for
the Degree of Master of Science

Milwaukee, Wisconsin

May 2024

ABSTRACT
DEVELOPING CONTINUOUS PREDICTIVE CONTROLS
FOR ANKLE ANGLE AND MOMENT ACROSS
MULTIPLE MOBILITY TASKS

John Eganhouse, B.S.

Marquette University, 2023

This thesis aimed to create a predictive model for controlling lower limb prostheses, using electrical activity from muscles in the residual limb to predict ankle angle and moment across mobility tasks including level ground walking, stair ascent, and descent (LW, SA, and SD). In aim 1, kinematic and kinetic ankle data, were used together with electromyographic (EMG) signals obtained from six healthy ambulators to train a nonlinear autoregressive (NARX) model to predict ankle angle and moment. Networks were trained with a delay of 58.33 ms, using a 120 ms sampling window and tested for their ability to predict ankle angle and moment across mobility tasks using a 10-fold cross validation. The average root-mean-squared error (RMSE) of networks across tasks was 2.93°±0.70° and 0.12±0.03 Nm/Kg when shank velocity was provided as input, 4.92◦±1.39° and 0.15±0.04 Nm/Kg when EMG activity was provided as input, and 2.37°±0.58° and 0.084±0.026 Nm/Kg when inputs were combined. In Aim 2, the best performing networks were tested in a modified version of a model of the Marquette powered prosthetic foot. Three cases were considered: open-loop NARX prediction with internal feedback and closed-loop NARX prediction that used either ankle angle feedback, or ankle angle and moment feedback from the prosthetic model. The internal feedback model accurately predicted its target without incorporating information from prosthetic foot performance. Simulations that incorporated modelled moment feedback increased error, causing instability over time in some SA and SD trials from a mismatch in desired and achieved ankle moment.

The NARX networks in Aim 1 accurately predicted ankle angle and moment across subjects and mobility tasks and could be used to provide kinematic/kinetic control input for a powered prosthesis. In Aim 2, the subsequent control simulation performed well with internal feedback, but full closed-loop validation requires an updated model that incorporates loading and ground reaction forces. The system's potential for real-time operation without conscious input is promising. Future work should explore human-in-the-loop control performance and testing with amputee data, to characterize the impact of individual sources of variability associated with changes in residual muscle signals, adaptation over time, and diverse movement patterns.

ACKNOWLEDGEMENT

John Eganhouse, B.S.

I would like to thank Dr. Scott Beardsley, my committee chair and thesis advisor. Dr. Beardsley was instrumental during every step of the way: from helping to identifying my thesis problem statement, advising my course work to cater to my thesis, to helping drive the direction in my research, and guidance through the process of writing my thesis. I consider him a mentor as a researcher and as a person. I would also like to thank Dr. Erika Zabre-Gonzalez for the use of her test subject data, for intruction on neural network development, and other thesis advisement.

I would like to thank the other members of my thesis committee, Dr. Jordan Williams and Dr. Philip Voglewede. Their comments on my thesis improved its content, especially in developing more purpose and context into the background literature review. Dr. Voglewede's input was especially important in the conception of my research, helping Dr. Beardsley and myself identify a problem statement to address in this thesis as well as ideas in going about developing my research.

Finally, I would like to thank my parents Joseph and Patrica Eganhouse for their support and encouragement through my time in graduate school.

TABLE OF CONTENTS

LIST OF TABLES

LIST OF FIGURES

I. INTRODUCTION AND BACKGROUND

1.1 Problem Statement and Introduction to Aims

The purpose of this research is to create a predictive transtibial control system that provides continuous predictions of ankle kinetics and kinematics across different mobility tasks. Various control schemes have been proposed for actuated lower limb prostheses with the goal of improving gait in amputees. However, the goal of prosthetics, to provide robust real-world function to restore gait which is intuitive to use, remains elusive. Discrete control of continuous gait profiles has emerged as a primary means of providing user-control across different terrains and mobility tasks. However, it has inherent limitations in its ability to respond quickly to external perturbations and/or conscious changes in gait strategy based on environmental conditions and to smoothly transition between mobility tasks (i.e, walking to stair ascent) in real-time. In the literature, prosthesis control that combines the above-mentioned features remains absent and the union of them is imperative to achieve full rehabilitation for a lower limb amputee. Accurate prediction of continuous movement across mobility tasks could address these gaps and improve the usability of lower-extremity prostheses.

Toward this goal, two specific aims were pursued that centered on the development and testing of a predictive transtibial control system that operates seamlessly across different mobility tasks. Each aim is divided into sections discussing the significance, rationale, approach, results, and their implications toward robust lower-limb prosthesis control. Within each aim, key factors are underscored to highlight their significance as design outcomes toward the overall goal.

1.1.1 Aim 1 - Develop a Recurrent Model of Gait, Capable of Predicting Joint Kinetics and Kinematics Across Mobility Tasks

To develop a control system that continuously drives the ankle angle and moment of a transtibial powered prosthesis across mobility tasks, a machine learning approach will be used to train networks to predict ankle angle and moment using external inputs to ensure accurate and on-time actuation of the prosthesis. The proposed system will incorporate the following features:

Predict ahead of time – The network will predict ankle angle and moment ahead of time in the sagittal plane. The networks will do so by relating current predicted values to past predictions as well as current and past external inputs. Prediction ahead of time is needed to account for transitions and to allow for lagless motor actuation of the prosthetic device.

Function across tasks – This predictive network must work across different mobility tasks including walking, stair use, and their transitions.

Provide continuous control– The networks will continuously update the driving signals to the prosthesis to ensure timely response to external disruptions to gait.

Incorporate real-world inputs– The network must predict future ankle kinetics and kinematics using input from sensors that can be reasonably incorporated into an existing prosthetic design.

Have low error – The primary measure of performance will be to minimize the root mean squared error (RMSE) of ankle angle and moment across the gait interval compared to target timeseries.

1.1.2 Aim 2 - Test the Recurrent Model in Conjunction with an Existing Prosthetic Control Model

To validate the predictive network developed in Aim 1, the subject-specific trained networks will be incorporated into a real time computer model of prosthetic movement and motor actuation. The ability to maintain stable and accurate movement with the combined system (the existing control model and additional predictive network) will provide proof-of-concept for the predictive network approach to prosthesis control. The combined system will do the following things:

Incorporate physiological and prosthetic inputs – The intended state of the prosthesis will be monitored using a combination of physiologic (electromyographic (EMG)) signals and embedded prosthetic sensors.

Provide stable control in response to model feedback – The response of the predictive model must remain stable in response to feedback from estimated (rather than true) ankle kinetics and kinematics.

1.2 Background

1.2.1 Human Gait Adaptation and Amputee Challenges

Adaptation is important to human gait and it occurs both over short time and long time scales. When walking, transitioning between directions can occur almost instantly and new terrains, angles, obstacles, and other walking contexts can be adjusted over short time scales (in seconds) (Choi & Bastian, 2007). Additionally, it has been found that leg movement adaptation occurs independently for each leg (Choi & Bastian, 2007). Humans possess the ability to adapt their walking patterns across terrain types and to remain stable in a largely automatic/unconscious manner (Kannape & Herr, 2016). The motor systems of the brain can adapt rapidly to internal goals, external factors, and

training (Pearson, 2000) and the rhythmic nature of gait can help enforce learning of motor patterns. This automatic and largely unconscious adaptation in movement is central to everyday life. It is an important capacity to restore during rehabilitation and restoration of gait in lower limb amputees, and therefore in the development of active prosthesis.

1.2.2 Types of Lower Limb Prosthetics

Modern lower limb prostheses encompass a wide range of devices designed to assist lower limb amputees. Various terms are used to describe such devices based on the type of amputation they are designed to accommodate, such as 'transfemoral' for an above knee amputation and 'transtibial' for below the knee amputation that passes through the tibia. This thesis focuses on aspects of prostheses related to transtibial designs.

Prosthesis can further be subdivided into passive and active (or powered) prosthesis. While the roots of modern lower limb prosthetic technology extend deep into medical history, the definition that will be used for "modern" lower limb prosthetic technology starts at the solid ankle cushioned heel (SACH) foot. The SACH foot was approved for production in 1957 and is still important today in rehabilitation and it serves as inspiration for newer prosthetic designs.

1.2.3 Passive Prostheses

Passive prostheses are those which do not provide additional energy during use. They can be non-elastic or incorporate energy storage and return (ESR or ESAR) elements to better mimic the energy return of the ankle during walking. The solid ankle cushioned heel (SACH) foot is a common example of a relatively inexpensive non-elastic

prosthesis used by people who do a limited amount of walking (Hansen et al., 2016). As the name suggests, the SACH foot cushions the impact of the foot hitting the ground, which is important for joint health and walking endurance, but it does not provide energy return during liftoff of the foot. Other passive foot prostheses exist such as the SAFE (stationary attachment flexible endoskeletal) which is like the SACH foot but accommodates inversion and eversion motion (Hansen et al., 2016), enabling the foot to turn into or away from the midline of the body which can help with stability on uneven surfaces.

Although passive prostheses aid tremendously in rehabilitation, walking still requires the input of mechanical energy from the body and any mechanical energy lost through the prosthesis requires the user to compensate, resulting in greater than normal energy expenditure by the user due to the loss in mechanical efficiency. The amount of energy input is low for slow walking but gradually increases with speed leading to a noticeable decline in the mechanical efficiency of passive prosthesis. Compensating for this issue often causes other parts of the body to take on atypical forces and/or movement, which can lead to suboptimal walking patterns such as leg swinging (Hansen et al., 2016). In a study conducted by Sinitski et al. (E. H. Sinitski et al., 2012), the gap in efficiency for stair ascent and descent between healthy limbed subjects and passive prosthesis aided subjects was found to be significant. Pelvic rotation was greatly increased as amputees swung their leg out more instead of moving primarily in the sagittal plane to ensure ground clearance (P. F. Su et al., 2008).

Increased energy usage and suboptimal movement patterns can make walking with a non-elastic prosthetic ankle more fatiguing than with an intact leg and can result in

injury over time due to repetitive overexertion and atypical loading of the remaining joints during compensatory movements (E. Sinitski et al., 2022). Moreover, asymmetrical movement enhances the possibility of fatigue, strain, or injury over time. Minimum foot clearance (MFC) in relation to trips and falls has been found to vary across different movement tasks (Loverro et al., 2013), indicating a need for different movement (and control) profiles across mobility tasks such as walking, stair ascent, or stair descent) . Protopapadaki et al. (Protopapadaki et al., 2007) support this concept, showing significant differences in hip and knee angles and moments between stair ascent and descent.

Energy storage and return (ESR) prosthetic systems, sometimes called dynamic-response prostheses, store kinetic energy from early stance (starting at heel strike), via a spring compression, and release the energy in late stance (ending at toe off) (Hansen et al., 2016). ESR systems help mitigate the extra effort an amputee must put into each step by returning energy to the movement in a way that mimics the elastic properties of a natural foot and its tendons. While this energy return has the primary effect of increasing rehabilitated movement, some ESR systems have been shown to also reduce impact forces and stresses on the side of the intact foot and leg (Hansen et al., 2016). However, ESR prostheses are still not equivalent to an intact foot due to the lack of active power input which is needed to achieve appropriate torque at the ankle. Additionally, ESR feet cannot actively compensate for obstacles in the way an intact foot can, due in part to the lack of external power (Gardiner et al., 2016).

1.2.4 Finite State Powered Prosthesis Control

More recently, various types of active/powered prosthetic systems have been developed for use with lower and upper extremity amputees (for a broader review of the state of the art see (Gehlhar et al., 2023)). Lower limb active/powered prostheses are sometimes referred to as microprocessor feet due to their reliance on onboard computing (Hansen et al., 2016). Unlike passive systems, powered prostheses require an actuator with a control system to exert forces that coincide with the user's gait cycle to mimic the dynamics of the intact limb. Finite state control models enable the implementation of different control modes across tasks within a single automatic control scheme (Sun et al., 2014). In finite state control, each gait cycle is broken down into distinct phases e.g., heel strike, foot flat, etc. that cascade together during normal gait, and are augmented by data received at key foot contact events and from measurements of joint velocity (Sun et al., 2014). Finite state control allows for the modulation of gait speed and adaptation to changes in terrain slope (Hansen et al., 2016). However, such systems typically rely on an expectation of continued cyclical gait events or do not account for multiple types of mobility tasks. For example, when changing to a new locomotive task, such as ascending stairs, the user must begin the first step before the prosthesis can recognize the change in task and adjust the timing and application of power appropriately.

Increasingly finite state models are being developed to function across multiple mobility tasks. Some prostheses, such as the BioM developed by Hugh Herr and the MIT Media Lab, have integrated finite state control with partial volitional EMG control; see Figure 1 for a concept diagram (Kannape & Herr, 2014). During the toe-off phase of gait, the BioM uses control signals that are proportional to muscle activity measured by surface electrodes to adjust the lift of the foot. The incorporation of voluntary user input

from muscle activity to dynamically adjust the prosthesis's performance is referred to as volitional control. Incorporating proportional volitional control increased the power of the prosthesis's output during key parts of foot lift off but did not attain the full power expected from normal ambulation of two intact legs. In spite of this, the performance with volitional control came close in power output to that observed in normal ambulation, which could make it a viable option for stair ascent with a prosthetic limb given further tuning. However, expanding volitional control in a finite state model increases the complexity of the model and testing process. For instance, each new mobility task (e.g., stair ascent) requires the development of a new finite state control and processes for switching between all available states.

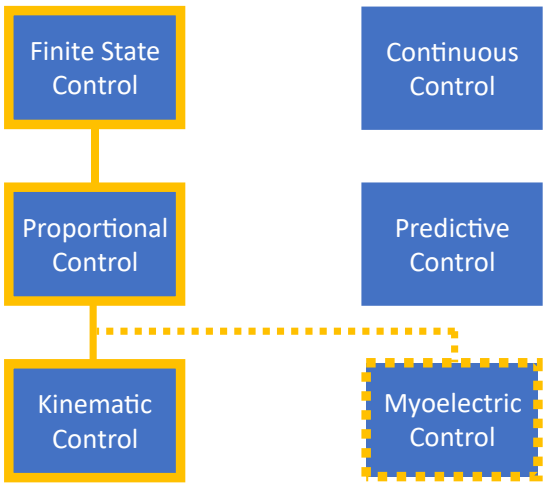

Figure 1: Finite State Model with Additional Proportional Control
This figure shows a concept level representation of the main approaches used for prosthesis control. At the highest level is the approach for implementing control, finite state (I.e., discrete) or continuous control. The second level addresses the timing of the control, whether it is proportional (current time step) or predictive (future time step). The third level addresses the type of feedback that can be incorporated from the prosthesis/user. The yellow outline denotes an example of a specific control scheme that implements a finite state model with proportional kinematic control, with optional myoelectric input.

Other studies have combined finite state control with proportional control to actuating foot lift during stair ascension (Kannape & Herr, 2014). Hoover et al. developed a transfemoral linear two-state impedance control (Hoover et al., 2013), that used proportional myoelectric signals (I.e., surface electrical activity from muscles) to modulate knee trajectory during stair ascent. In contrast to Hoover's proportional myoelectric control, Au et al. used myoelectric sensing of muscle flexion to aid in the transition between two finite state controllers (Au et al., 2008). Another finite state model is developed by Grimmer et al. for the Walk-Run ankle; a walking and running model that controls from standing to walking and running, as well as their transitions (Grimmer et al., 2016). It adjusts motor position based on the current gait more, gait speed, and gait cycle progression percentage by mimicking healthy subject reference data. It was found that the model performed well for walking identifying a speed of 1.6 m/s, slightly overshot the identified speed for 2.6 m/s running by 0.2 m/s, and slightly undershot the 4.0 m/s running case by 0.3 m/s. In these studies, myoelectric control is shown to be possible in a finite state model, but the challenge is to integrate it state by state whereas a continuous control method could integrate myoelectric input through the entire control scheme.

1.2.5 Continuous and Myoelectric Control in Powered Prostheses

During continuous control, the output of the powered prosthesis is directly related to the input signal, often through a PID control (Proportional-Integrated-Derivative). Unlike finite state models which rigidly progress through phases of gait cycles, continuous control does not use defined phases or states. During continuous myoelectric proportional control, the action taken by the prosthesis scales directly with the intensity

of the muscle activity measured with EMG. Compared to the finite state model with volitional control which only used proportional myoelectric control in one aspect of gait, continuous myoelectric proportional control is fully reliant on the amplitude of the EMG signal(s) throughout the gait cycle.

Upper limb prosthetic systems have used continuous myoelectric control, but typically require training to learn how to consciously activate the requisite muscle groups and master the timing of activation (Kuiken et al., 2009). Huang et al. found that lower limb amputees could use the electrical activity of residual muscles for continuous proportional control of a powered prosthesis in a controlled treadmill environment. They noted that visual feedback on a screen was needed in their test to generate a significantly higher peak power (S. Huang et al., 2016). Other than that, continuous myoelectric control has not been widely studied in the context of lower limb prostheses but has been more so applied to upper limb prostheses. One possible reason is that active conscious control of lower limb movement is not a natural way to walk. The process of walking is automated (subconsciously) to a much greater extent than upper limb movement. Furthermore, unlike for upper limb control, making mistakes in lower limb control will lead to tripping. When developing a lower limb prosthesis, there is a need to replicate the unconscious nature of use while avoiding tripping. Precision in automation is difficult when talking about something as complex as fully rehabilitating movement. Full rehabilitation with proportional myoelectric control would require a great deal of sophistication, device tuning, and user learning.

1.2.6 Pattern Classifier Models in Prosthetic Control

Pattern classifier models use patterns in the input signals to prompt a system response, in which case the user must be trained to replicate those patterns. Pattern classifier models occupy a middle ground for prosthesis control and have been more extensively developed in the context of upper limb prostheses. In these systems, the patterns of activated muscles and their relative intensities are used to determine the user's intended movement (Kuiken et al., 2009). This method can achieve more seamless conscious control by matching signals to a fixed set of movement patterns (Kuiken et al., 2009). Pattern classifier-based approaches enable more complex control compared to proportional control but do not eliminate the need for conscious control by the user which may make it less suitable for lower limb prostheses.

1.2.7 Myoelectric Feedback as Predictive Signals.

Myoelectric prediction leverages the coupling between neuro-muscular activity and the generation of muscle force and the corresponding delay to obtain an electrical signal that is predictive of joint kinematics. This type of data is most readily collected from surface EMG (sEMG) sensors placed on the skin above a muscle group and can be obtained from residual muscles within socket to predict and control a transtibial prosthesis (Farmer et al., 2014). Silver-Thorn and colleagues (Silver-Thorn et al., 2012), showed that independent muscle contractions still occur in the residual limb while walking with a prosthesis over multiple gait cycles. The access to residual muscle activity (through sensing of sEMGs) gives an opportunity to measure myoelectric signals within the p. Furthermore, subjects could be quickly trained to strengthen activation of residual limb muscle during gait, allowing for an avenue of trained myoelectric control.

1.2.8 Continuous Predictive Control

Continuous predictive control is the concept of controlling across multiple mobility tasks such as walking, stair ascent, and descent without the need for switching control strategies. This type of continuous control could provide a more seamless approach, whereby future movement is predicted based on previous kinematic and myoelectric data, (Farmer et al., 2014). The approach leverages the cyclic patterns of lower extremity movement, similar to pattern recognition (due to a built-in reliance on previous kinematics) and could provide seamless user control during different types of gait and their transitions. Continuous predictive control has the benefit of adding user intent, like proportional control, while predicting ahead of time to compensate for lags between sending a control signal and actuating the motor to achieve a desired angle and moment.

Training a predictive network could reduce the burden of user adaptation by tuning the network to the user's own movement and muscle activation patterns. Finally, due to the nature of a trained network being adapted to a desired set of movements, it removes the need to map new segments of gait into incorporate new forms of movement such as stair ascent. The quality of the network revolves around the chosen network structure and quality of the input data. Neither of these factors need to incorporate the specific phases of a gait cycle or any other model behavior to function. With a trained predictive network mode, it is not necessary to implement new control states, as with a finite state model, to accommodate new types of movement. Instead, the model structure can remain fixed and additional training data added that incorporates the desired movement.

In this thesis, a predictive control system is developed around a nonlinear autoregressive neural network that incorporates external inputs (i.e., a nonlinear autoregressive model with exogenous inputs (NARX)). NARX networks can be trained to predict a continuous signal based on a set of continuous inputs. These types of algorithms leverage machine learning to make semi-random adjustments to a network's weights to minimize the error of the predicted output (compared to a set of known 'true' values). Once trained, the network functions in the same way as a traditional autoregressive moving average network (Braun, 2001).

To contextualize the plan to develop a predictive control system using NARX networks the following is a review of much of the state-of-the-art research in that field with the most similar applications. An example of a study conducted using continuous prediction of movement data was performed by Dey et al (Dey et al., 2019). During the study, ankle angle and moment during walking were continuously predicted using a vector regression model whose inputs were hip and knee joint motion data. When the model was applied to self-selected walking speeds, the correlations between actual and predicted ankle angle and moment were high (R^2 = 0.98 and .97 for angle and moment respectively). Eslmay and Alipour (Eslamy & Alipour, 2018) showed that ankle shank angle and angular velocity could be used to estimate ankle angle and moment across multiple walking speeds though a gaussian process regression. Haung et al. (H. Huang et al., 2009) also found that EMG signals can be used to classify patterns of locomotion/mobility tasks. In a study of eight able-bodied subjects and two long transfemoral (lt) amputees, 10 electrode placements on the musculature above the knee were shown to differentiate between four phases of gait with errors ranging between 5.2

and 12.4%. Huihui and colleagues (Huihui et al., 2018) demonstrated that sEMG mean, variance, and waveform length could be used to estimate ankle angle using a combined feature fusion and random forest approach for network optimization. Similar to the approach taken in this work, (Prasertsakul et al., 2012) showed that a nonlinear autoregressive model with exogenous inputs (NARX) could be used to predict knee and ankle movement when using myoelectric data from eight lower limb muscles.

Most recently in the study of myoelectric lower limb prosthetic control, (Keleş & Yucesoy, 2020) used combinations of five different EMG signals (tibialis anterior, medial gastrocnemius, rectus femoris, biceps femoris, and gluteus maximus) to predict ankle angle and moment for able bodied subjects during level ground walking. Studies have also been conducted to compare the relative merits of different types of machine trained networks in predicting joint torque and found a positive correlation with actual torque predicting 0.4 seconds ahead using long short-term memory neural networks (LSTM) from four able bodied subjects standing, walking, running, and sprinting at self-selected speeds on a treadmill with RMSE averaging 0.08 N*m / Kg for the LSTM networks somewhat shifted to a lower RMSE by their standing results (Siu et al., 2021). Further experiments in the prediction of multiple mobility tasks have been published averaging 2.38 to 5.45 degrees RMSE (Gupta et al., 2020). These findings further add support to the viability of EMG inputs for designing prosthetic control schemes.

1.3 Background in Relation to Aims

1.3.1 Aim 1

In Aim 1, a continuous myoelectric predictive network is developed to predict ankle angle and moment across multiple mobility tasks. Accounting for multiple

mobility tasks has always presented a problem for finite state control. While additional control states can be readily incorporated, the process of predicting and transitioning between states (i.e., mobility tasks) remains a challenge. Our approach addresses both limitations by developing a model that directly relates continuous changes in EMG activity to changes in ankle angle and moment. By employing the user's natural patterns of EMG activity to predict future ankle state, our approach will address system lag and avoid the need for conscious control that is inherent to most proportional control systems. The added significance to the field of study will be the continuous control during the transitions between mobility tasks as well as the combination of myoelectric and kinematic inputs in a predictive model could help reduce overall error.

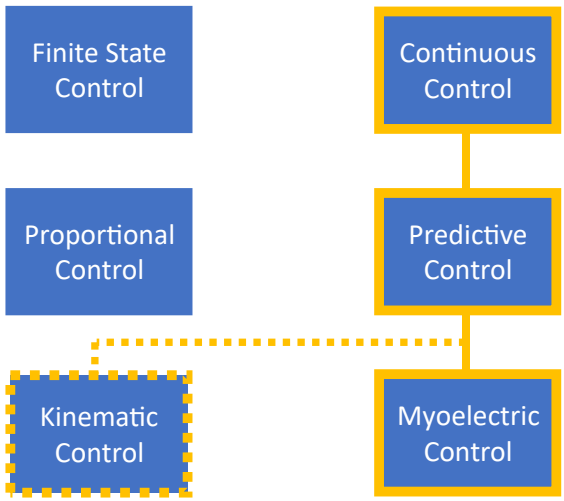

Figure 2: Narx Control System
This figure shows a concept level representation of the main options in prosthesis control that form the basis for the NARX network developed as part of the research.

1.3.2 Aim 2

The purpose of the second aim is to test the feasibility of the myoelectric predictive network developed in Aim 1 for real time control of a transtibial prosthetic

device. To achieve this aim, a proof-of-concept test model developed around an existing Marquette powered prosthesis will be used to show that the NARX model can provide a stable control signal. A computer model that takes in an input data stream while simultaneously predicting and controlling a prosthetic model will bring us one step closer to the final design. Prosthesis control simulations in literature also don't incorporate continuous predictive controls.

II. AIM 1

1. Introduction

In aim 1, a continuous myoelectric predictive network is developed to predict ankle angle and moment across multiple mobility tasks. A series of network models is examined that vary based on the type of inputs available to the model (kinetic, kinematic, and myoelectric) and the structure of the underlying nonlinear autoregressive (NARX) model. No other types of networks besides NARX are tested in this thesis. The predictive qualities of each model are measured based on predictive error to a novel set of gait profiles that includes transitions between different types of gait (walking, stair ascent, etc.). One area of significance to the literature is that most studies do not address the challenges associated with continuous control between (and across) mobility tasks. Task transitions can be difficult to account for with finite state methods. Furthermore, the combination of myoelectric and kinematic inputs in a predictive model could help reduce overall error compared to a network using only one of the two types of inputs. The hypothesis being that each type of input contributes different information to the prediction. A benefit is expected in predicting mobility task transitions with myoelectric data since previous kinematic/motion data does not predict future changes in motion, it only aids in predicting that the past cyclic motion will continue.

2. Methods

2.1 Ambulation Data

Training data was selected from a previously acquired subject data set (Zabre-Gonzalez et al., 2021). The gait profiles of six healthy ambulators were selected for training and testing the predictive model. The data for each subject included 10 trials (9 used for training and 1 held back for testing) of simultaneously collected EMG, and kinematic and kinetic measures of gait across three mobility tasks (level-ground walking, stair ascent, stair descent, and their transitions). Subjects had an average age of 21.9 ± 1.4 years (mass 72.5 ± 8.8 kg, and height 1.8 ± 0.09 m). EMG (i.e., myoelectric) data was collected at 1200 Hz using Trigno™ electrodes placed bilaterally on the tibialis anterior, medial gastrocnemius, and the lateral gastrocnemius. Myoelectric data were then down sampled to 120 HZ to match the subject's kinematic data and were processed to extract the low frequency linear envelope of the high frequency EMG signal. Simultaneously with EMG signals, 3D joint position (kinematic) data were collected using a 16-camera OptiTrak motion capture system, and ground reaction forces/moments (kinetic data) were obtained using four 6-DOF force plates embedded in the floor and stairway which is used in calculating the ankle moment target over time. Movements were recorded for three mobility tasks: level ground walking, stair ascent, and stair descent. Stair ascent and descent trials contained two steps of level ground walking combined with two full sets of left/right steps on the instrumented stairway. The average trial length varied between level ground walking (1.21 s), stair ascent (3.58 s), and stair descent (3.33 s). Additional details regarding the experimental setup and data collection can be found in (Zabre-Gonzalez et al., 2021).

2.2 Training/Test Data

The kinematic and kinetic data from the six ambulators (ankle angle and moment over time data calculated from motion capture data and the embedded force plates) were used to train subject-specific models to predict the intended ankle movement across mobility tasks. To facilitate model training, shank velocity (i.e., velocity of the tibia) was extracted from the motion capture data and used as a substitute for on-board accelerometer data that would be collected from a transtibial prosthesis. Velocity was chosen instead of acceleration as a movement metric for training to reduce noise associated with the derivative calculations applied to the motion tracking position data. Conversely, in a physical system, calculating velocity from accelerometer data (by integrating acceleration over time) would tend to smooth the movement data. For training the predictive model, the measured ankle angle and moment were specified as the model target output, and the EMG and shank velocity data were defined as the model input. Each subject specific model was trained using 9 of the 10 trials (randomly selected) from each of the three mobility tasks. The remaining trial from each mobility task was held back from training and used to independently test the generalization performance of the trained model.

To test the stability of different types of network configurations (i.e., number of hidden units, duration of sampling window and prediction intervals, etc.) and optimize the network structure, a single (typical) subject out of the six was selected for preliminary training/testing. Then, the best performing network structure was used to train and test a separate predictive model for each subject.

2.3 NARX Networks

The predictive model was based on a nonlinear autoregressive neural network with exogenous input (NARX), which was used to map the past and current measurements of EMG and shank velocity to future (in time) values of ankle angle and moment during gait. The term "neural network" refers to the process used to optimize the model performance by adapting the weights connecting network nodes based on a supervised learning algorithm as seen in Figure 3.

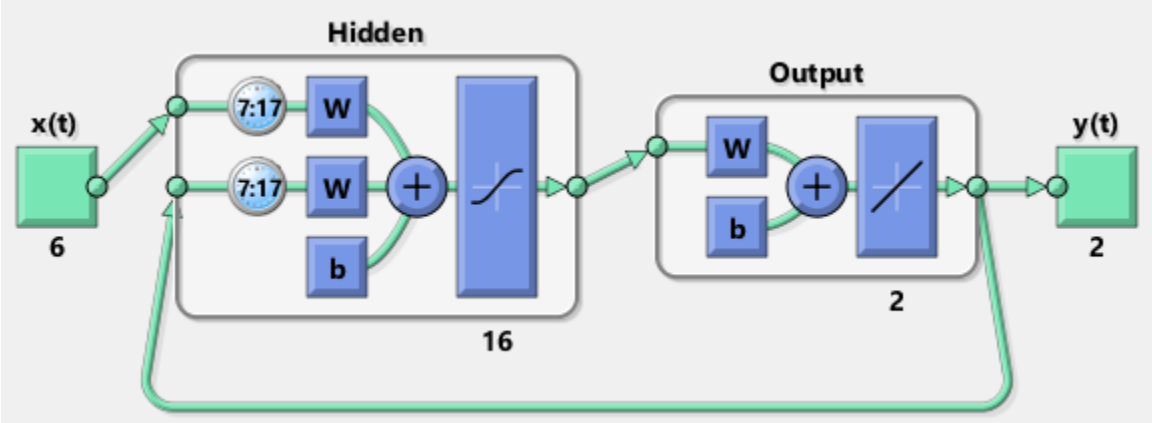

Figure 3: "Closed-loop" NARX Network Structure
The network input x(t) consisted of six timeseries (3 EMG + 3D shank velocity) presented within a moving 10-sample window and the network output, y(t), reflected the timeseries for ankle angle and moment, predicted seven timesteps ahead of the current time point. The hidden layer contained 16 units with sigmoid transfer functions and the output layer contained two units with linear transfer functions.

Once the network was trained, it functioned as a normal autoregressive model. The NARX models were initialized and trained using MATLAB's neural network "Deep Learning Toolbox" (R2019a MATLAB version 9.6 and Deep Learning Toolbox version 12.1). Each network consisted of a single hidden layer of nonlinear nodes which receives inputs from a sample window of previous (delayed) data points and prior model outputs,

and a linear output layer trained to predict the future ankle angle and moment. The optimal values for input and feedback delays were examined in this study briefly with reference to previous work (Zabre-Gonzalez et al., 2021) and used as the basis for selecting the NARX model parameters. The NARX model structure used for final training/testing included 16 hidden units, an input delay of seven timesteps (58.33 ms) and a ten timestep (120 ms) prediction interval. Other model parameters tested included training functions, transfer functions, and training exit criteria but had minimal effect on the model performance. The model weights were trained using the Levenberg-Marquardt algorithm, which is also the default in MATLAB, to optimize the model performance by minimizing the least-squares error between the measured values of ankle angle and moment and the model predictions of ankle angle and moment.

2.4 Closed Loop Networks

These networks were trained as closed-loop networks which means they did not use the true ankle angle and moment as feedback to the input layer. The only feedback the model could directly incorporate was the input (which acts as indirect feedback) and the recurrent feedback of the model's previous predictions. In other words, they were closed to external feedback. In general, closed networks tend to be less accurate but are more robust to variations in input data they receive.

2.5 Training Set-up

The main way that network training results were impacted was by manipulating the structure of the data input into the networks during training. Various combinations of inputs were examined including two to three EMG inputs with and without 3D shank velocity. The inputs were always matched against the "real" expected ankle angle and

moment recorded from the 3D motion capture system mentioned in section 2.1. Separate networks were trained using only EMG data, only shank velocity data, or both as inputs to characterize the relative contributions of each input source to the overall model performance. In all training permutations, networks were trained by sampling whole trials rather than randomly sampled points. This whole trial sampling was done to ensure that an equal amount of level ground walking, stair ascent, and stair descent data was used to avoid biases in training error minimization. The specific MATLAB NARX model properties used during training were divideFnc = 'divideblock', dividemode = 'sample', trainingRatio = 0.80, valRatio = 0.20, testRatio = 0, such that 80% of the training data was used optimize the model weights, and the remaining 20% of the training data was used to validate the generalizability of the weight changes. Additionally, during training both angle and moment data were normalized to ensure an equal contribution to the error minimization process.

2.6 Cross Validation

Each subject-specific model was trained and tested using a 10-fold cross-validation strategy to ensure that all trials were evaluated for generalizability. During training, a single set of trials (one from each mobility task) was withheld for testing that network's performance on novel data. In other words, for every network configuration that was generated, ten different networks which had all seen a slightly different subset of nine from the total ten data sets (and a unique set of novel trial data to assess performance) were trained and saved.

For each training/test 'fold', ten separate models were trained, each with randomized initial weights and the best performing network was selected for each fold.

Finally, the errors in predicted ankle angle and moment were averaged across the 10-folds to characterize the overall performance of the predictive model. This process helped to minimize the likelihood of randomly seeded network weights leading to non-optimal network performance; such bad performance as from a local minimum trap, where the network training ceases early due to reaching the training parameter maximum iterations of failed error improvement or one of the other criteria outline in section 2.7.

2.7 Training Evaluation Criteria

The performance criteria used in the MATLAB training was a normalized combination of angle RMSE and moment RMSE averaged over the whole trial. The training of each network halted after failing six consecutive validations, wherein the weight changes applied to the model increased the error on the validation data. Alternatively, one of the other default training exit conditions could be met to end early, such as minimum performance gradient. Lastly, training could exit due to meeting the error goal, but this did not occur since the error goal was set to zero.

2.8 Input Permutations

The difference in most of the network types tested was the content of the inputs to the network. Networks were trained with inputs consisting of only 3D shank velocity, only myoelectric data, or a combination of both. These network permutations were trained to assess the necessity and complementary nature of the inputs towards predicting ankle angle and moment. As indicated in Section 2.4, all networks used the real ankle angle and moment for the purpose of training but as closed networks they were not allowed to access this information as feedback to predict future estimates of ankle angle and moment. This input limitation was done for multiple reasons. First, open-loop

network training was found to create networks with unstable predictions due to the disconnect between the model predictions and unchanging ‘true’ kinematic, kinetic, and myoelectric data. In a real system this data would change in response to network output providing active feedback, but this effect cannot be replicated in training. Second, target kinetic and kinematic data were not assumed to be accessible signals whereas myoelectric and accelerometer data could be relied on with a system implemented with surface electrodes.

For networks trained using shank velocity data, the model received three inputs corresponding to the three dimensions of shank velocity. The networks were trained against the real ankle angle and moment but when performance was evaluated for the test trial the model was only provided with shank velocity as the external input. Networks with only velocity inputs were trained to evaluate the sole predictive qualities of previous movement data for predicting future kinematics and kinetics.

Networks that were reliant only on myoelectric inputs were trained on either two or all three of the EMG signals recorded from the tibialis anterior, medial gastrocnemius, and lateral gastrocnemius. EMG only trained networks were created to evaluate the sole predictive qualities of EMG data.

Finally, networks were trained with combinations of 3D shank velocity and myoelectric data resulting in five or six inputs depending on whether 2 or 3 EMG inputs were used. This was done to evaluate the complementary nature of shank velocity and myoelectric data.

2.9 Network Analysis

Once a network was trained its ability to predict ankle angle and moment was evaluated using the withheld set of level walking, stair ascent, and stair descent 'test' trials. Several metrics were used to evaluate the trained network performance. First, the neural network performance metrics defined within the neural network toolbox were compared based on the average normalized combined error of angle and moment. Second, average RMSE was calculated for each mobility task (level walking, ascent, and descent) as well as the RMSE across all task types. Third, prediction vs the target time series were plotted for comparison and evaluated with respect to their time series correlation.

3. Results

3.1 Network Type Comparison on a Single Subject

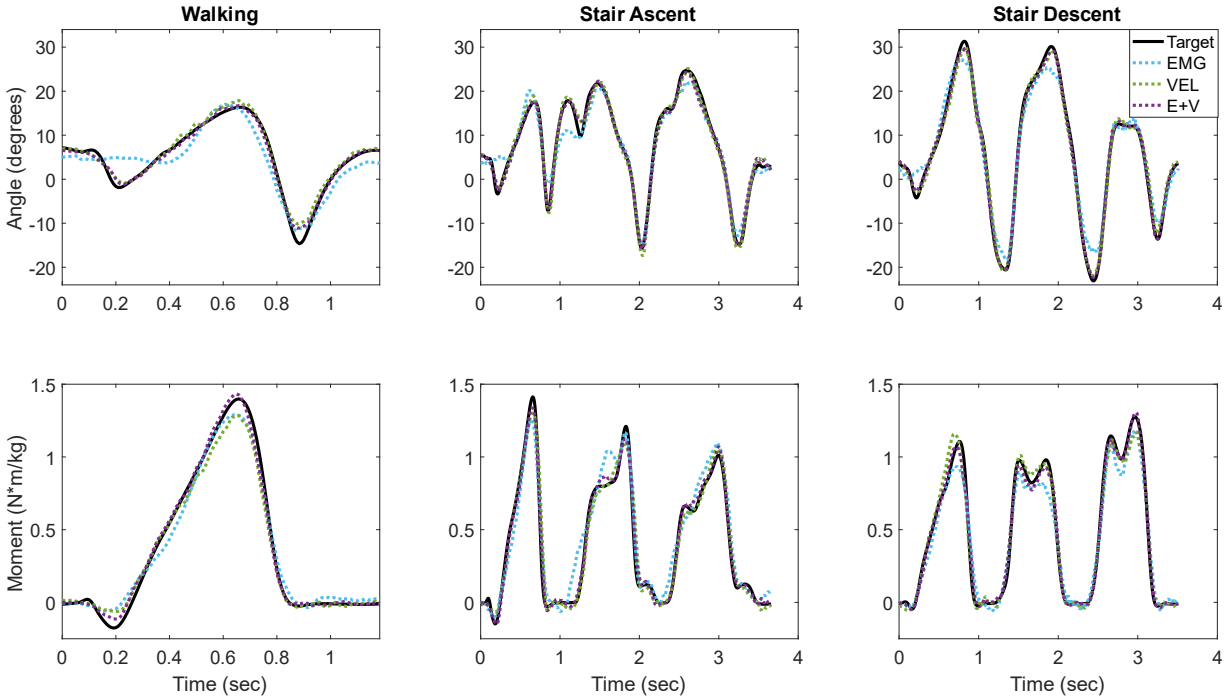

Figure 4: Prediction vs target ankle angle and moment across task type.
Average angle and moment predictions are shown for Subject #5 using networks trained with EMG only (EMG; blue), velocity only (VEL; green), or both (E+V; purple) inputs. Model predictions are shown for level ground walking, stair ascent, and stair descent from left to right. The averaged target profile (average of 10 trials) is denoted by the solid black line.

Figure 4 shows the predicted ankle angle and moment profiles averaged across the 10-fold cross-validation for each mobility task (walking, stair ascent, and descent) as a function of the type of input (EMG only, velocity only (VEL), or EMG and velocity (E+V)) used to train the NARX model. The average target profile (across the 10 trials) for each task is shown for comparison. On average, E+V trained networks most closely

predicted ankle angle and moment profiles across tasks followed by VEL and EMG trained networks respectively.

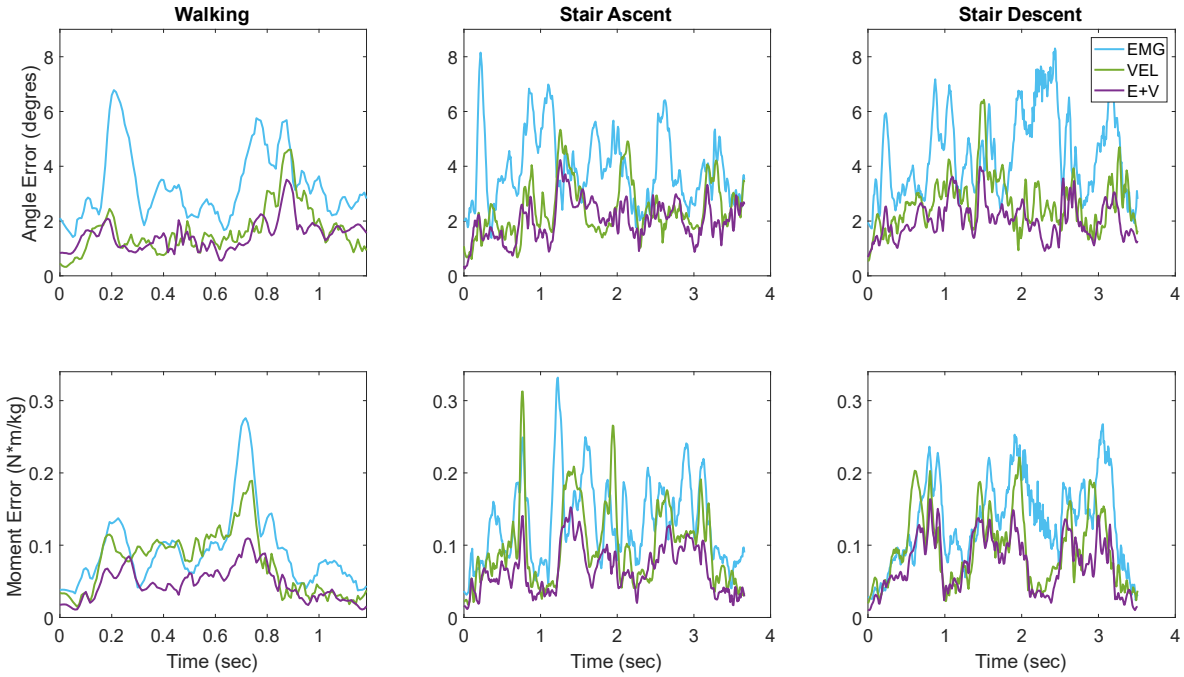

Figure 5: Average absolute error over time across mobility tasks.
Average absolute error over time for angle angle and moment for a typical subject (Subject #5) using networks trained with EMG only (EMG; blue), velocity only (VEL; green), or both (E+V; purple inputs. Model errors are shown for level ground walking, stair ascent, and stair descent from left to right.

Figure 5 shows the absolute error over time between the model and target profiles averaged across the 10-folds. Average error over time was consistently lowest for E+V trained networks. The average error of VEL trained networks was sporatically lower at times as seen in the graph, especially in the walking condition and at the beginning of the angle prediction. The average error spiked at certain time points but was not consistent between network types, although there are certainly areas of similar error highs and lows. Usually, error spikes corresponded to the prediction failing to hit target peaks or

lags/leads in sharp curves. Particularly there is lower error at the begining and end generally, which is due to those time points being more deterministic in the experimental set up because each trial starts and ends in the same phase.

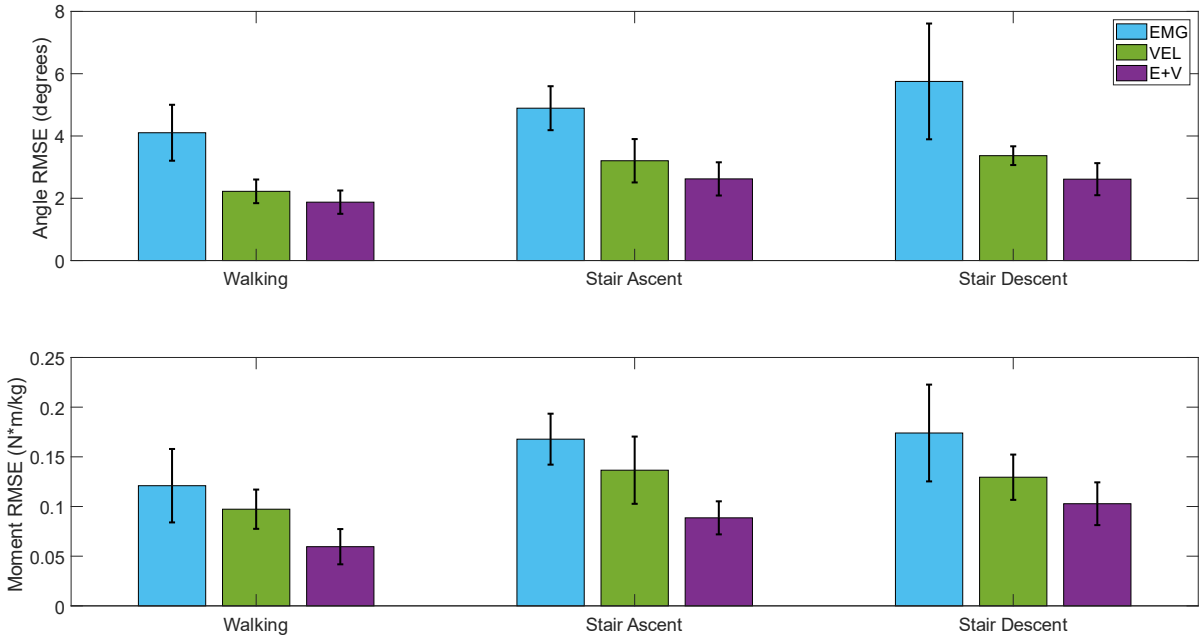

Figure 6: Average RMSE across networks and task types.
RMSE of ankle angle and moment for EMG, VEL, and E+V (Subject #5) trained networks averaged across the 10 training/test folds for Walking, Stair Ascent and Stair Descent trials. Error bars denbote ± 1 SD.

The RMSE of ankle angle and moment averaged across the 10 test folds is shown in Figure 3 for the three mobility tasks. The average error for both angle and moment shows is lowest for the walking, followed by stair ascent, and stair descent. However, the angle prediction of E+V shows little difference between stair ascent and descent in average RMSE. Additionally, the moment prediction of VEL nets is also similar between stair and descent on average in terms of RMSE.

3.2 Cross Subject Comparison

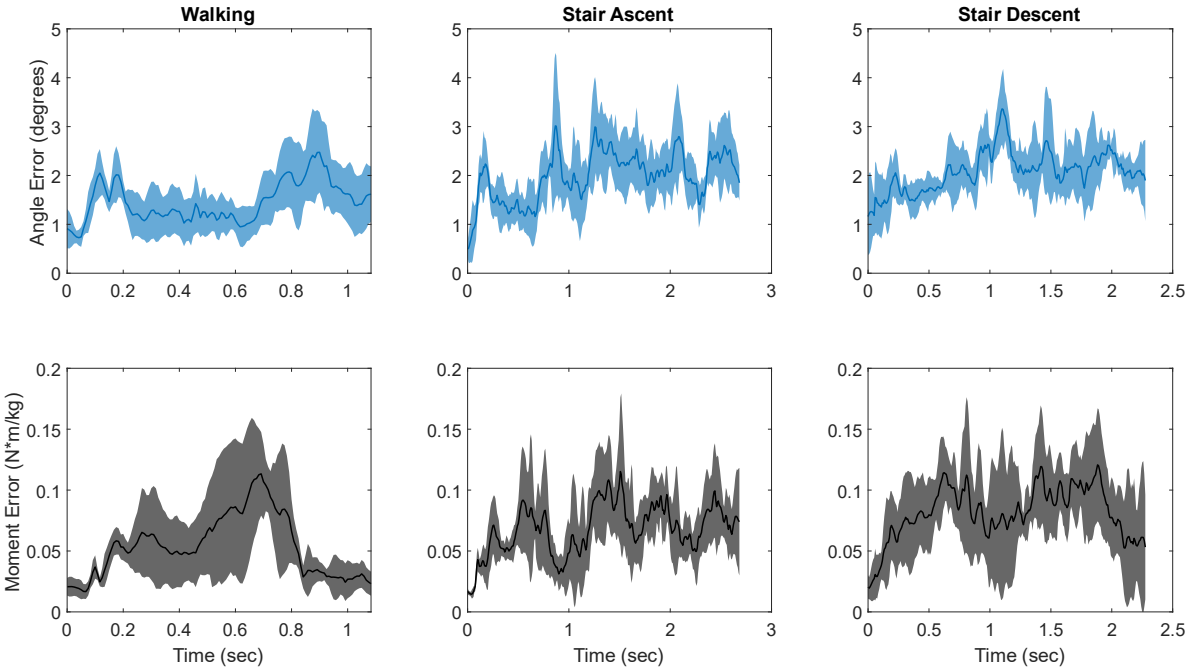

Figure 7: E+V absolute error of ankle angle and moment over time across subjects Absolute error over time averaged across six subjects (solid line) for networks trained with E+V inputs. Columns correspond to the error in ankle angle (top row) and ankle moment (bottom row) for the three mobility tasks. The shaded region in each plot corresponds to ±1 SD.

The absolute error over time averaged across subjects of E+V trained networks is shown in Figure 7. The average error in ankle angle across subjects was less than 2.5 degrees during walking and less than 3.5 degrees for stair ascent and descent. The average error in ankle moment was consistent across mobility tasks (<0.125 N-m/kg).

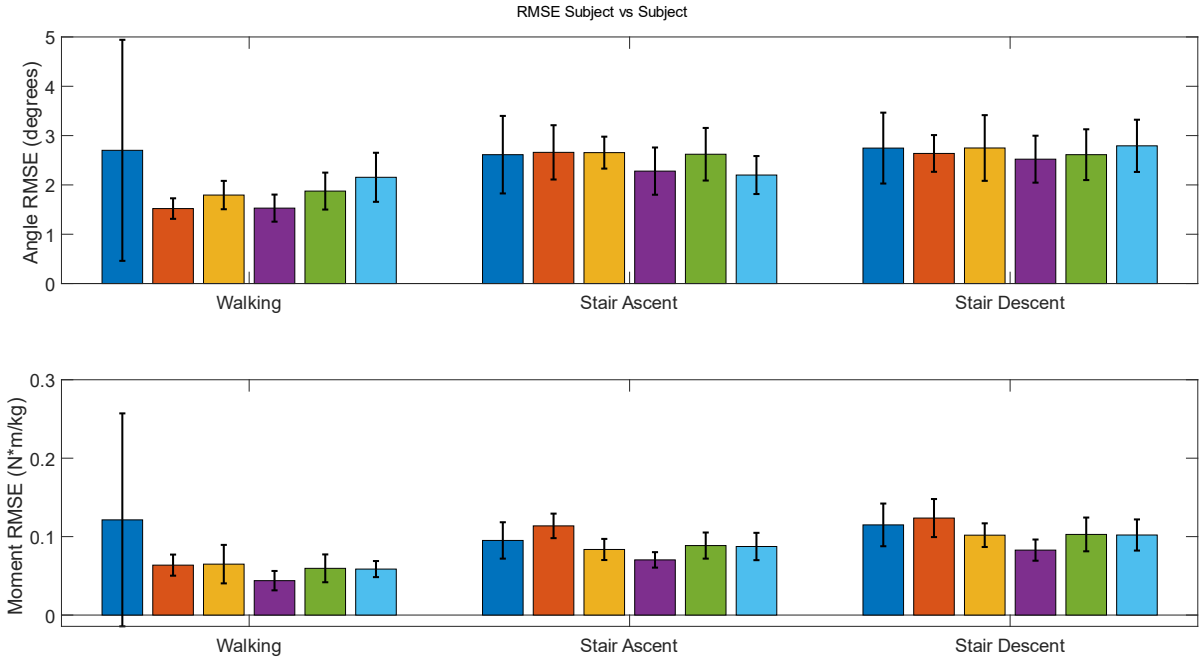

Figure 8: RMSE across the gait cycle for each subject and task type for networks trained with E+V inputs.
Ankle angle (top row) and moment (bottom row) RMSE across the gait cycle for subjects 1-6 (colored bars left to right by task) for networks trained with E+V inputs. Error bars indicate ±1 SD. Each colored line represents a different subject.

Figure 8 shows the RMSE across the gait cycle for each subject. It is noteworthy that subject 1 (blue) had an abnormally high error trial during walking which drove the increase in the mean and standard deviation. Otherwise, the predictive networks performed similarly across subjects within each mobility task in terms of RMSE. Subject 4 consistently had the lowest RMSE across tasks for both ankle angle and moment. Subject 5 (green) had the most representative RMSE across subjects and was the example subject used in the comparison between EMG, VEL, and E+V networks. Some anomalous behavior is seen as subject 1 (blue) has a particularly bad prediction on 1 of 10 trials affecting the whole average. This anomalous trial performed poorly in angle and moment but more so in moment.

4. Discussion

4.1 Principles/Relationships/Generalizations

4.1.1 Closed Loop Networks

The results demonstrate that a closed-loop nonlinear autoregressive network can be trained to accurately predict ankle angle and moment from myoelectric, kinetic, and kinematic inputs across mobility tasks (level ground walking, stair ascent, and stair descent) and their transitions. The performance of networks combining myoelectric (EMG), and velocity (VEL) inputs performed better than for networks using either set of inputs alone. The average error across trials for E+V networks was lower for every task, with a RMSE of 2.37 degrees and 0.0837 N*m/kg for ankle angle and moment respectively. In addition, the network correlation to the target was higher on average and had better error versus range of motion ratio. RMSE versus range of motion gives context to the error values of angle, comparing the error to the extent a joint is moving in the data.

4.1.2 Impact of Network Input Structure

In general, velocity trained networks performed better than myoelectric trained networks across mobility tasks. The RMSE of velocity trained networks was 39.62% lower for ankle angle and 21.41% lower for predictions of ankle moment. The average standard deviation of RMSE across trials was also lower in velocity only networks. However, E+V networks performed best with RMSE 20.81% and 30.88% lower than velocity trained networks for ankle angle and moment respectively.

The improvement in performance stems from the complimentary nature of the two input signals but it is worth examining the differences between the two sets of inputs. Myoelectric data is a measure of the electrical activity of muscle and contains electrical

signals that necessarily precede the generation of muscle force and limb movement. Shank velocity data (measured at the midpoint between the knee and ankle) does not contain a predictive signal with respect to the underlying biomechanics. It can signal cyclic movements well, but it does poorly in predicting limb adjustments made during the transition from one task to another.

There are several reasons that velocity may have improved performance over myoelectric input alone despite not containing information about subject intent. First, shank velocity has a higher signal to noise ratio compared to myoelectric inputs. In a prosthetic system, the integration of shank acceleration, vis-à-vis accelerometers, to measure velocity could act to reduce the contribution of random noise across the time series and further increase the signal to noise ratio. This factor was not able to be exploited in this case but could further improve performance in real system implementation. In contrast however, velocity measures based on differentiation of sampled position data (such as from a motion capture system) may increase noise. Despite the possibility for higher noise, the signal to noise ratio of the shank velocity inputs derived from the motion capture system was still higher than the myoelectric (EMG) inputs to the network.

Second, regardless of how shank velocity was computed, the velocity measurements were less affected by motion artifacts (unlike the EMG data). In both cases motion artifacts can occur when the position of the sensor (or in the case of motion capture, the position of a marker) moves. The difference is that during movement, non-isometric muscle contraction will cause movement of the muscle relative to the skin that will shift the position of the surface EMG electrode relative to the muscle being

measured. The physical shift manifests as motion artifacts that are highly coupled to the task-related EMG inputs and can be challenging to remove from the underlying data. Motion artifacts due to shifts in the sensor the surface of the skin can also occur, but the movement of the muscle due to contraction is unavoidable and ever present.

A third factor is that the muscle activity measured with EMG is derived from a summation of all electrical impulses measurable from the skin surface and may contain elements that are not correlated to the muscle contractions controlling the movement of the ankle. The final reason velocity networks can outperform EMG networks is that the trials being trained on are highly regular. When comparing trials of the same task type, such as level ground walking, there is relatively low inter-trial variance. EMG's advantage of reflecting a subject's intent matter less when movement is cyclical, and the subject's intent does not reflect an unanticipated change in movement. The more similar gait intervals are, the more each individual trial resembles one period of a repeating cyclical profile. It stands to reason that under more non-cyclical conditions, the performance gap based on the type of network input (EMG vs. shank velocity) would shrink or may even flip so that EMG networks were more advantageous. The experimental set up that produced the training data was chosen to measure a variety of movement types and transitions but was constrained in its complexity by the instrumentation used to obtain the kinetic and kinematic data and standardization of the tasks across subjects. Therefore, in the current datasets the amount of time where user intent to modify gait is relevant represents a relatively small portion of the total training data. In other words, the time interval where future intent matters in these trials is small relative to the portions where it is cyclical.

In general, providing more inputs to a model does not necessarily lead to a better model prediction, however, here the complimentary nature of the shank velocity and EMG inputs lead to significantly better performance overall. As discussed previously, shank velocity inputs have a high SNR signal and can facilitate the prediction of cyclic movements that are common during gate while myoelectric inputs provide information regarding cyclic gait *and* subject intent. Other contributing factors to the non-redundancy of the data are that that there is a time differential between the onset of both signals and the fact that the muscle activity being measured did not directly cause the movement of the shank itself.

With respect to the mobility tasks, all networks performed best for walking conditions in terms of average RMSE even though the total training time for walking trials was lower (the walking trials represent less total time of gait). This is not a surprise due to the lower complexity in the ankle angle and moment profiles and the lower range of motion (RoM) over time, but it's worth noting that the trend held across all configurations of the network inputs. The design of the network training was influenced by the concern that overspecification to a specific task type could occur when different tasks are represented by unequal amounts of total time. This difference in total time could become problematic if the training was performed in the default mode of randomly sampling time points across the training data. Random sampling would not guarantee that all gait trials (and types of gait) were equally represented. Therefore, training was done on entire gait trials using the same number of trials for each task type. This did not mean that training time was equivalent between task trials just that the training ratios were held constant. The bias towards walking trials in terms of average RMSE can be

explained in part by their lower target variance even though the total training time on walking trials was lower.

Similarly, E+V networks had the highest correlation in each task type for both angle and moment. Input type did have a differential impact on correlations of angle and moment predictions. EMG only trained networks was the worst and velocity was the best in terms of RMSE and correlation but E+V had virtually no bias either compared to EMG in terms of correlation. Between task type correlation bias and angle/moment bias E+V wins. The lack of bias between the variables in trial prediction is a good indication that the networks performance was reaching a ceiling with an average Pearson correlation coefficient of .976 for ankle angle and .986 for ankle moment across all task types.

4.1.3 Adjustments to Network Size

As outlined in the methods, a network node count of 16 was chosen based on the lack of a substantive impact of larger networks on performance during preliminary testing. The RMSE exhibited a nonlinear asymptotic decrease as the size of the network (i.e., number of nodes in the network) increased up to 16 nodes and was approximately constant with 24 and 32 nodes. While average network RMSE was similar in the larger networks individual network performance was more variable, particularly for networks incorporating EMG inputs. As a result, the value of larger networks was considered questionable, and they were not examined further. However, it was unclear why a larger network does not translate into better performance. Since more nodes give a network more degrees of freedom, it is possible that the model prediction was under-constrained. When networks are under-constrained the weights in each node can become too well fit to the training data. This over-specification to the trained data typically hurts network

generalization to novel data. The use of a 10-fold cross validation during training helped to ensure that the optimal number of nodes was identified despite performance variations which can result from the random seeding of the initial training weights.

4.2 Exceptions

Predictions for EMG-based networks had relatively high errors at the start and end of trial predictions across task types. When trial variability over time was examined, the start and end points of trials for each task type were similar for ankle angle predictions. This outcome is reasonable since the start and stop points of each trial were defined based on heel strike resulting in similar foot positions. However, EMG-based networks consistently started out with 2 degrees of angle error across tasks as shown in Figure 5. In the walking condition, the E+V networks showed a similar onset error but yielded values that fell between EMG and velocity networks. During stair ascent and descent errors in E+V and velocity networks were similar. Despite the cyclic nature of the tasks, the parsing of gait into discrete trials resulted in onset transients due to the recursive structure of the network. In a practical application, where measures of ankle angle and moment are continuous over time, these onset transients would not be present in the network prediction.

4.3 Comparison to Previous Work

4.3.1 Myoelectric Predictive Networks

Keleş et al. examined the ability of a network trained with combinations of one to five surface EMG signals (tibialis anterior, medial gastrocnemius, rectus femoris, biceps femoris, and gluteus maximus) to predict ankle angle and moment for able bodied subjects (Keleş & Yucesoy, 2020). Their networks used 32 nodes with a nineteen-data-

point delay and did not predict beyond the next time point. Input combinations ranging from a single EMG up to all five EMGs were used to train the model and performance was ranked based on the number of EMG inputs. Networks trained with five EMG inputs were found to perform the best for level ground walking trials. In direct comparison to this work, the ankle error was comparable, but the addition of shank velocity improved prediction quality in terms of average RMSE. The ability to achieve comparable performance using fewer inputs makes for a simpler design solution. It may be possible that a larger set of EMG inputs (for example using high density EMG arrays) could yield better performance but at the expense of increasing complexity. To date, however, no studies have leveraged high density surface EMG arrays for myoelectric predictions of gait. To the extent that such arrays are used, the increase in performance may be limited due to correlations between electrodes and the additive noise contributions of each EMG signal.

In a separate study Zarshenas et al. used time delayed neural networks to predict ankle moment for exoskeleton control during level treadmill walking (Zarshenas et al., 2020). They compared networks designed to use EMG alone to predict ankle moment as well as networks that combined EMG and kinematic inputs. In addition to using larger network models (up to 40 nodes), their networks were trained to predict ankle moment up to 2 seconds into the future. They showed good prediction performance for cyclic walking. As expected, error rose with the prediction time interval but not as dramatically as might be expected (error typically rises the further a prediction is from the sample window). This lower error rise is likely tied to the cyclical nature of the walking task, which is more amenable to extrapolation. Although the result for their zero-time ahead

model (the closest result to our study) was good at 8.5% torque RMSE/ROM (range of motion), it was still worse compared to the E+V trained networks here whose average cross subject RMSE/ROM for the same condition (level ground walking) was 5.5%. The average torque RMSE/ROM for their EMG only network was 12.5% which is comparable to the performance of EMG trained networks here (11.6%). Interestingly their networks performed worse even though they were trained only on walking trials whereas here the networks were forced to generalize over three mobility tasks. The larger network structure may have hurt performance in the next timestep prediction (as opposed to the predictions 2 seconds into the future).

Other models have predicted joint torque for multiple gait profiles, from level ground walking to sprinting; using a variety of network structures including dense feedforward networks (6 layers with 80 hidden units), convolution neural networks, neural ODEs with 110 hidden units, and long short-term memory (LSTM) networks with 64 hidden units and 2 dense layers with 16 hidden units (Siu et al., 2021). Models trained with a combination of surface EMGs and accelerometer data showed good sequence-to-sequence prediction, the primary network test case for this work. A sequence-to-sequence prediction is where the entire prediction timeseries is computed in one batch based on an input timeseries. With the LSTM network, sequence to sequence performed the best with a moment RMSE of 0.08 N*m/kg for all activities and an average Pearson correlation of 0.88. The performance is similar, but the sequence used to predict gait required a substantially larger sample window. For future angle predictions (0.5 and 3s), an average activity RMSE of 0.09 N*m/kg and average correlation of 0.6735 was

achieved. Although the average error of future ankle angle remained similar to the regular sequence-to-sequence prediction, the correlation over time dropped dramatically.

Gupta R. et al. modelled continuous angular position of the ankle during unconstrained locomotion (level ground walking as well as ascent and descent of stairs and ramps) using a combination of surface EMG and knee joint angle inputs (Gupta et al., 2020). They used a similar NARX architecture and examined performance as a function of the network size (5 to 30 nodes) across delays ranging from 1 to 10 timesteps or 8.33 to 83.3ms. With a delay of 58.3ms, the same as in this study, the best performing network in the level ground walking condition was the 5-node network with an RMSE of approximately 11 degrees. With a one timestep delay, the model prediction improved and to levels consistent with the results reported here. They also found that the inclusion of knee angle greatly reduced performance. While the network structure was very similar to the one implemented here, the decreased performance might be attributed to addition of ramp ascent and descent during training which increased the variability between expected target patterns. The optimization reported with a node count of 5 suggests that a low node count may be preferable for these types of predictive networks.

4.3.2 Classifier Networks

Another approach to solving ankle prosthesis control is using classifier models. One such study (Young et al., 2014) used EMG and mechanical sensors to enhance intent recognition in powered lower limb prostheses, similar to the prediction of ankle angle and moment incorporated in the current model. They reported that the state transition error decreased by 12.2 – 18.4% over their original model. Convolution neural networks have also been used to predict the type of gait (walking, ascent and descent of ramp and stairs)

for a transfemoral prosthesis using inertial measurement units (B. Y. Su et al., 2019). The model achieved classification accuracies of 94.15% ± 3.04% for healthy ambulators and 89.23% ± 7.56% accuracy for transfemoral amputees, show a different way in using EMG as a control signal.

4.4 Implications of Findings

This study examined the use of a predictive networks architecture for closed-loop control of ankle angle and moment for use in a transtibial prosthesis. The capability of the system to be quickly optimized for the individual user and the ability to operate in real time without conscious input from the user could improve prosthesis control when coupled with robust prediction across different types of ambulation.

The finding that network performance was optimized with a relatively small (16 node) architecture could facilitate real time implementation within a larger control system. With fewer nodes in the network, fewer computations are required for each time step prediction. Compared to other approaches incorporating more complicated network structures, E+V networks consistently performed better across locomotion tasks and provided a forward time prediction that could be used to compensate for control system and motor actuation delays when implemented in a prosthesis. Finally, the combination of surface EMG with onboard accelerometry enables the use of fewer sensors which simplifies implementation within existing prosthesis control systems.

III. AIM 2

1. Introduction

The purpose of the second aim was to test the feasibility of incorporating the myoelectric predictive network developed in Aim 1 for control of a transtibial prosthetic device. A proof-of-concept control simulation based on the Marquette transtibial prosthesis was used to demonstrate that a closed-loop NARX network can provide a stable control signal for actuating prosthesis ankle angle and moment in real time. The proof-of-concept control simulation developed here takes an important next step toward implementation in a physical prosthesis and ultimately tests of human-in-the-loop control.

2. Methods

2.1 Preexisting Model

The simulation is based around a model of a transtibial prosthesis developed at Marquette University (Sun et al., 2014)(Klein, 2018), the Marquette Prosthesis II. The model simulates the ankle mechanism's dynamics approximated as a quasi-static system. In this quasi-static model the dynamics are calculated as static models over a sequence of small steps. The mode of control used for the model translates desired ankle angle and moment into commands to a motor interfaced with a torsional spring to move the ankle. Low-level control of motor position was implemented using a proportional-integral (PI) impedance controller (Klein, 2018). The original model used a time dependent function fit to the generalized profile of ankle position and torque vs time reported by Winter (Winter, 2009) and was run on MATLAB 2019a.

2.2 Modeling Variable Timeseries

To be used with the predictive model from Aim 1, the Marquette Prosthesis II control model was adapted to accept and test using novel timeseries data. MATLAB scripts were used to approximate a best fit function of the target gait data using the approach described by Klein for direct comparison (Klein, 2018). A range of level ground walking, stair ascent, and stair descent trials were tested for each subject to characterize the robustness of the model response and range of motion.

Testing for the original model developed by Klein was done on timeseries from each movement condition: level ground walking, stair ascent, and stair descent. Of the three types of movement stair descent had the largest range of motion, ranging from 36 to -27 degrees across all subjects which necessitated modifications to the Marquette model (Klein, 2018). The physical movement of the system is constrained by a four-bar mechanism which physically limited the range of ankle angle from 15 degrees positive and 60 degrees negative. Positive and negative ankle angles are defined relative to the reference ankle angle that occurs when the foot is perpendicular to the ankle shank. Initial tests revealed that the positive angle limit was not sufficient to accommodate the measured ankle angles obtained from subjects during stair descent. Based on the results of the initial range of motion tests, modifications were made to the four-bar mechanism to accommodate the appropriate range of motion in angle. The modification made to the bar length (L_3; Figure 9) reflected the smallest adjustment sufficient to achieve the positive 40 degree limit of positive ankle angles measured from subjects during stair descent trials (Aim 1).

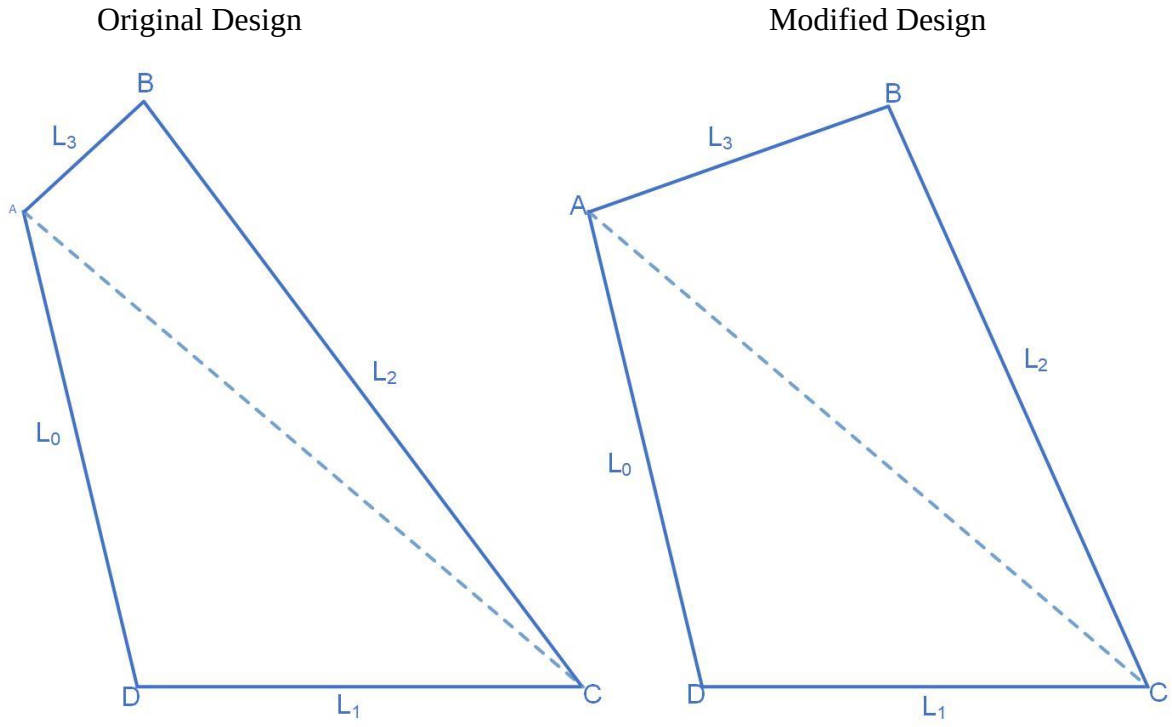

Figure 9: Modifications to the Four-bar Mechanism to accommodate the measured range of ankle angle.
In the original four-bar mechanism the model's torsional spring was attached at point A, the bar L_0 has the same orientation as the ankle shank, the bar L_1 has the same orientation as the foot and the angle at point D between L_0 and L_1 represents the ankle angle (measured relative to the perpendicular orientation of L_0 and L_1 such that a positive changes in angle reflected absolute angles less than 90 degrees. The dimensions of the original 4-bar mechanism were L_0 = 6 cm, L_1 = 5.48 cm, L_2 = 9 cm, and L_3 = 2 cm. In the modified design, the length of L_3 was increased to 4.3 cm.

2.3 Network Implementation

To fully model the control system, the NARX network (Figure 1) was incorporated into the modified prosthesis ankle model. Based on the results from Aim 1, E+V network was used with 6 inputs corresponding to the 3 EMGs and 3D shank velocity. The networks were incorporated into the Simulink model (R2019a Simulink Version 9.3) utilized the deep learning toolbox for Simulink. In the final implementation, the model was able to take EMG and velocity signals and control inputs and then

translate them first into motor output, and then ankle movement in accordance with the target angle and moment timeseries.

The open-loop control model used a static timeseries of angles and moments as input for the desired state. Then the desired inputs were translated into the desired motor position. Finally, the desired motor position was actuated using PI control.

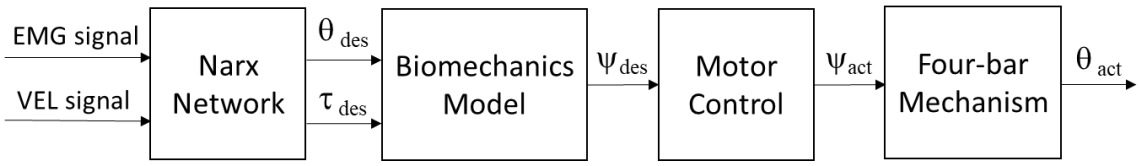

Figure 10: Marquette prosthesis open-loop control model for ankle angle with NARX prediction.
The NARX network takes in E+V signal input and outputs desired θ and τ. The outputs are fed into the biomechanics model that translates them to the desired motor position which is passed to the motor controller. Actuation of the motor translates results in a change in the motor joint angle Ψ which is translated into a change ankle angle θ via the four-bar mechanism.

When implementing the networks into the Simulink model, see Figure 10, the NARX network was trained to sample inputs and predict ankle angle/moment at 120 Hz. This sample rate differed from the variable runtime of the Simulink model itself which averaged a simulation rate that was approximately ten times faster. Due to this difference in sampling rates, the motor position was only updated when the NARX model had a new output (i.e., at 120 Hz).

2.4 Testing Across Task Types and Networks

The new NARX-Simulink model was tested separately using each subject's individually trained NARX model to predict ankle angle and moment across gait tasks. A MATLAB script was created to generate the network Simulink structure and modify

the primary simulation each time it was run. The simulation output was measured at a 120 Hz sampling rate and exported for analysis.

2.5 Testing with No Simulated Feedback

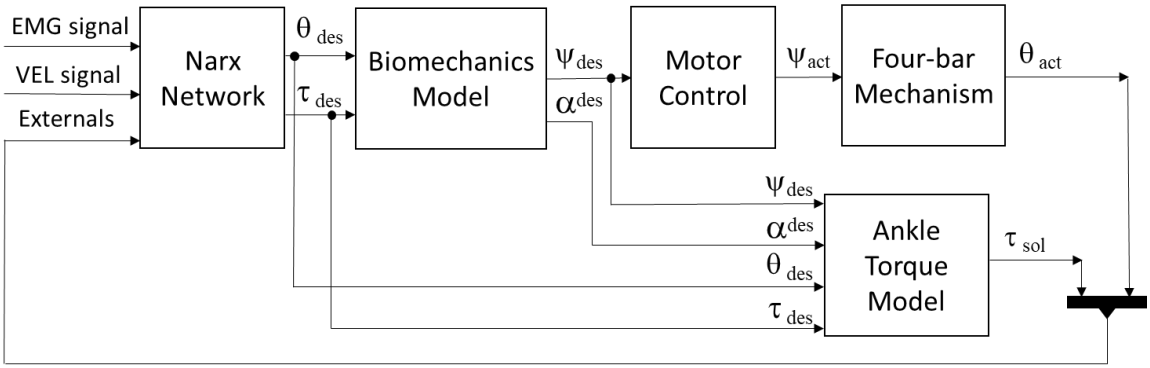

Figure 11: Maquette prosthesis closed loop control model with NARX prediction. The external feedback model has the same basic structure as Figure 8 but with the addition of the ankle torque estimator. The ankle torque model combines the desired y and desired a from the biomechanics model with the desired q and t from the NARX network. In addition, that NARX network can be configured to receive either the actual θ with and without the t estimate to account for the inability to directly measure ankle torque in the four-bar mechanism.

The NARX model itself is a closed-loop system that relies on internal feedback of the predicted angle and moment. External feedback in this context refers to feedback that occurs outside of the NARX model, which corresponded here to the feedback of ankle angle and moment of the simulated prosthesis. The performance of the full control model seen in Figure 11 was tested under two external feedback conditions. First, a test using only external feedback of the simulated prosthesis ankle angle was performed and then a second test was performed using external feedback of the simulated prosthesis ankle angle and moment. The testing was split into two conditions because the ankle angle can be read directly from the ankle joint prosthetic model; however, the applied torque could

not be computed without simulating the biomechanics of loading weight on to the joint during gait which was performed using a separate forward model. This divergent moment feedback resulted in an error characteristic that was not the same for angle and moment in the simulated model's output.

2.6 Evaluation Criteria

For the purposes of comparison, the outputs of the Simulink simulations were resampled to 120 Hz to match the data from Aim 1. The main measure used to test the success of the control simulation was the output ankle angle. For each task trial, the error between the simulation ankle angle and expected target angle was calculated as the absolute error over time and the average RMSE across task trials. Variability was quantified using standard deviation for each type of measured error. The average inter-subject error over time was also calculated using the average error trial for each subject.

3. Results

The control simulations based on NARX networks predictions of ankle angle and moment were successfully executed using the modified four bar mechanism dimensions. Results are reported below for three simulated control conditions: 1) NARX predictions based on internal estimates of ankle angle and moment, 2) NARX predictions based on external estimates of ankle angle and internal estimates of ankle moment, and 3) NARX predictions based on external estimates of both ankle angle and moment.

3.1 Control Model Performance Based on Internal NARX model feedback

Figure 10 shows the control system performance average across subjects when the NARX model predictions were based on internal feedback of the NARX estimates for

ankle angle and moment. In this condition the control system did not "see" the target timeseries.

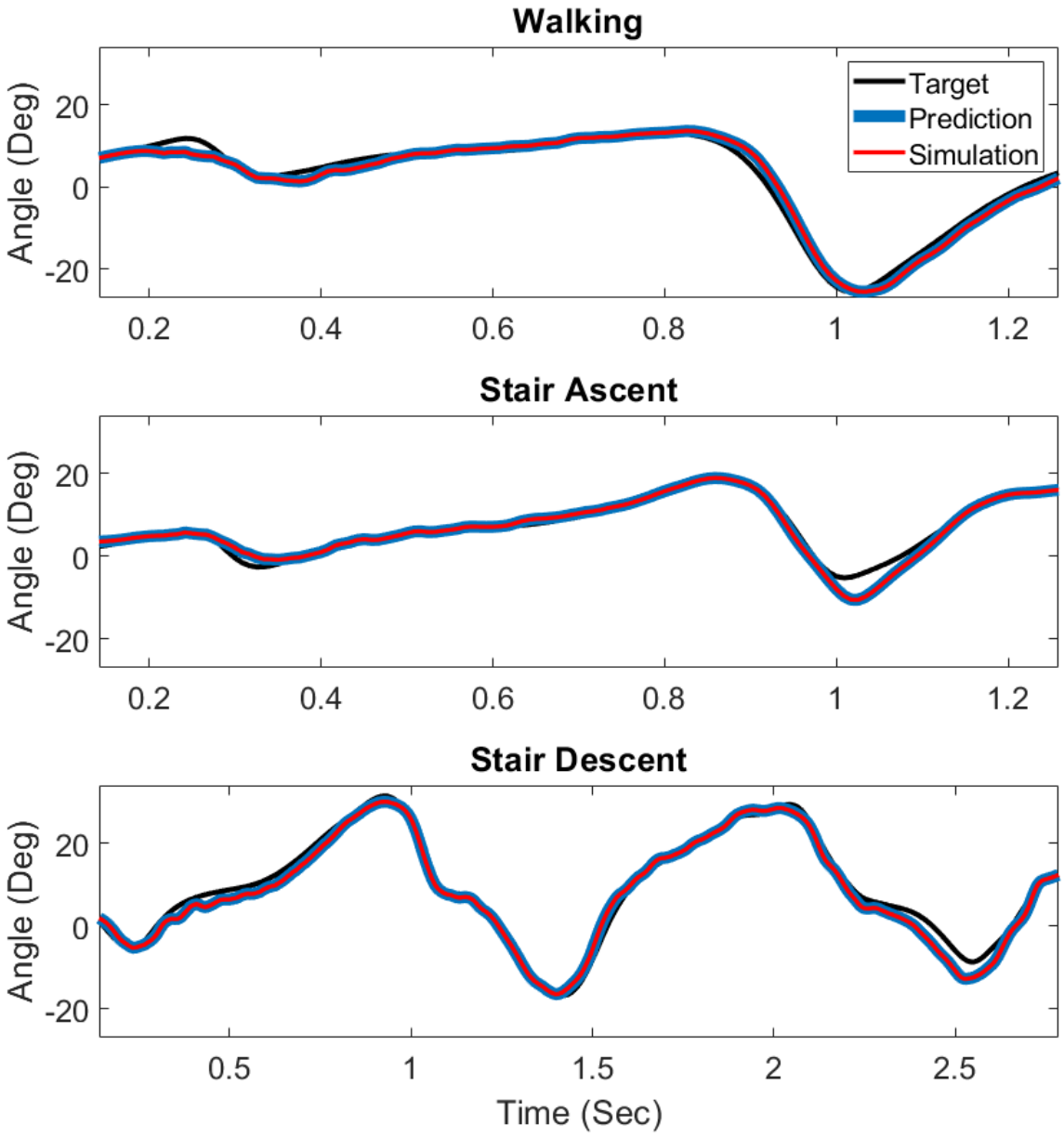

Figure 12: Maquette prosthesis closed loop control model with NARX prediction. The average target profile is shown in black, the average NARX prediction is shown in blue and the average control simulation ankle angle output is shown in red.

The difference between the NARX prediction and the control simulation over time was low across all task types. The error relative to average target was also low and

resulted predominantly from an slight lag or lead in the trajectory profile over time. The average RMSE of across trials was 1.93 ± 0.65 degrees for walking, 2.51 ± 0.51 degrees for stair ascent, and 2.68 ± 0.55 degrees for stair descent. The average RMSE between the NARX prediction vs the control simulation output was $3.38*10^{-4} \pm 3.14*10^{-5}$ degrees for walking, $8.53*10^{-4} \pm 8.37*10^{-5}$ degrees for stair ascent, and $1.03*10^{-3} \pm 1.09*10^{-4}$ degrees for stair descent.

Figure 12 shows the absolute error over time for all comparisons. The error between the target and the NARX prediction as well as the target and the control simulation are virtually identical. This lack of divergence is further illustrated by the near zero error between the outputs of the NARX prediction and control simulation over time.

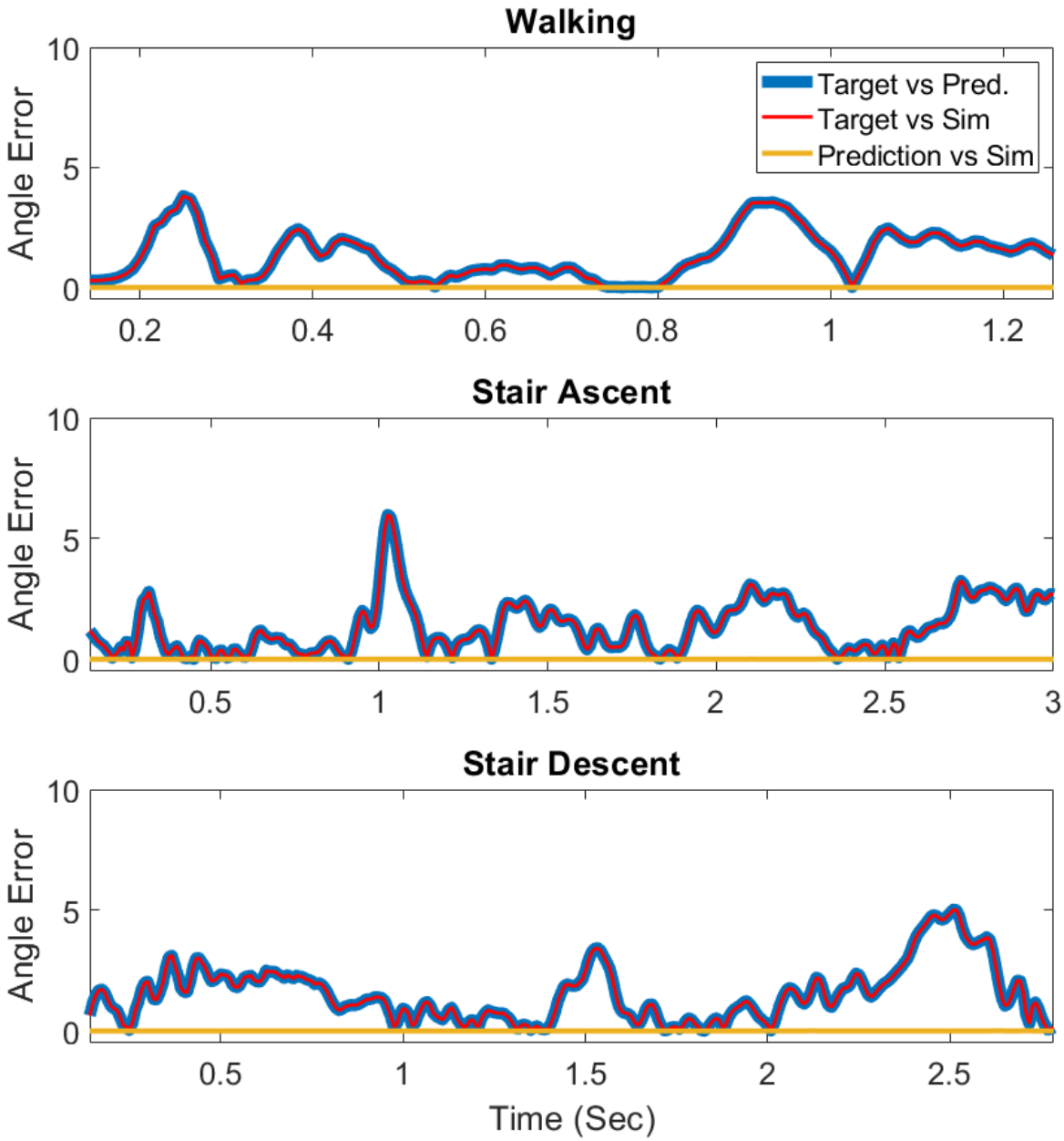

Figure 13: Average absolute error of closed-loop control simulation across task types. The blue line shows the error between NARX prediction and the target profile. The red line shows the error between the control simulation and the target profile and the yellow line shows the error between the NARX prediction and control simulation output.

The average error of the the prediction and the output to the target went to zero at several points typically corresponding to areas with a lack of lag or with high similarity

among training trials. The spikes correspond to areas of consistent lags or leads in prediction.

Table 1: RMSE (in degrees) of the control simulation ankle angle relative to the target timeseries across subjects and task types.

	RMSE				SD			
Subject	Walking	Ascent	Descent	Average	Walking	Ascent	Descent	Average
1	2.70	2.61	2.75	2.69	2.24	0.79	0.72	1.25
2	1.52	2.66	2.64	2.27	0.21	0.55	0.37	0.38
3	1.79	2.65	2.75	2.40	0.29	0.32	0.67	0.43
4	1.53	2.28	2.52	2.11	0.27	0.48	0.48	0.41
5	1.87	2.62	2.61	2.37	0.37	0.53	0.51	0.47
6	2.15	2.20	2.79	2.38	0.50	0.39	0.53	0.47
Average	1.93	2.51	2.68	2.37	0.65	0.51	0.55	0.57

In Table 1 the average RMSE across subjects and task types was 2.37 ± 0.57 degrees. This average RMSE is very similar to the NARX prediction performance.

Table 2: RMSE (in degrees) of the control simulation ankle angle relative to the NARX prediction across subjects and task types.

	RMSE				SD			
Subject	Walking	Ascent	Descent	Average	Walking	Ascent	Descent	Average
1	0.000394	0.000848	0.001153	0.000799	0.000033	0.000051	0.000200	0.000095
2	0.000255	0.000707	0.000819	0.000594	0.000015	0.000057	0.000055	0.000042
3	0.000313	0.000903	0.000959	0.000725	0.000027	0.000119	0.000116	0.000087
4	0.000353	0.000808	0.001063	0.000741	0.000034	0.000098	0.000073	0.000068
5	0.000323	0.000951	0.001090	0.000788	0.000035	0.000106	0.000077	0.000073
6	0.000389	0.000902	0.001074	0.000789	0.000045	0.000071	0.000133	0.000083
Average	0.000338	0.000853	0.001026	0.000739	0.000031	0.000084	0.000109	0.000075

Table 2 shows that the error between the simulated results and the NARX prediction is very low, almost non-existent. This holds across all mobility tasks, averaged across subjects.

3.2 Control Performance with Partial External Feedback

In the first set of control simulations, the control system was feedforward because the predictive networks used internal feedback. For the second set of control simulations, a hybrid closed-loop model was used where the ankle angle resulting from the control and simulated prosthesis was fed back to the to the NARX model. The ankle moment continued to be taken from internal feedback within the NARX model because it was directly measurable from the simulated ankle joint, but the model's moment estimate did not account for ground force interactions. The results for these simulations were nearly identical to the open-loop control simulations, those of the internal feedback system. The low error in the actuation seems to make no observable difference in accuracy of ankle angle across the gait tasks.

3.3 Control Model Performance Based on External Feedback

The full external feedback control simulation incorporated feedback from simulated prosthesis resultant ankle angle and moment. The moment produced by the system was calculated separately from mechanical ankle simulation based on the original control model for the Marquette prosthesis. This secondary torque calculation was done because the Simulink model was not sophisticated enough to produce an accurate torque response at the ankle joint. Direct model measurement of torque would have required a model that simulated real-time loading on the ankle joint. In its current form, the moment model represents a static loading of the ankle. However, the ankle torque solution produced by the model did not fit the torque profiles obtained from the experimental data. Therefore, it was anticipated that the control simulation performance would be less stable over time.

Table 3: Average number of open-loop simulation failures across task types due to control instability.

Failures	Walking	Ascent	Descent	Average
Average	0.0	3.3	4.2	2.5

A failure is a trial that failed to simulate to the completion of its timeseries. As seen in Table 3, there was surprisingly not enough instability to cause failures across subjects for level ground walking trials. There was a bifurcation in the stair ascent trials such that half the subjects had 1-2 failures (out of 10) and the other half had 5-6 failures. Stair descent control simulations had the most failures averaging 4.2 failures per subject with one subject's profiles resulting in 8 out of 10 failures.

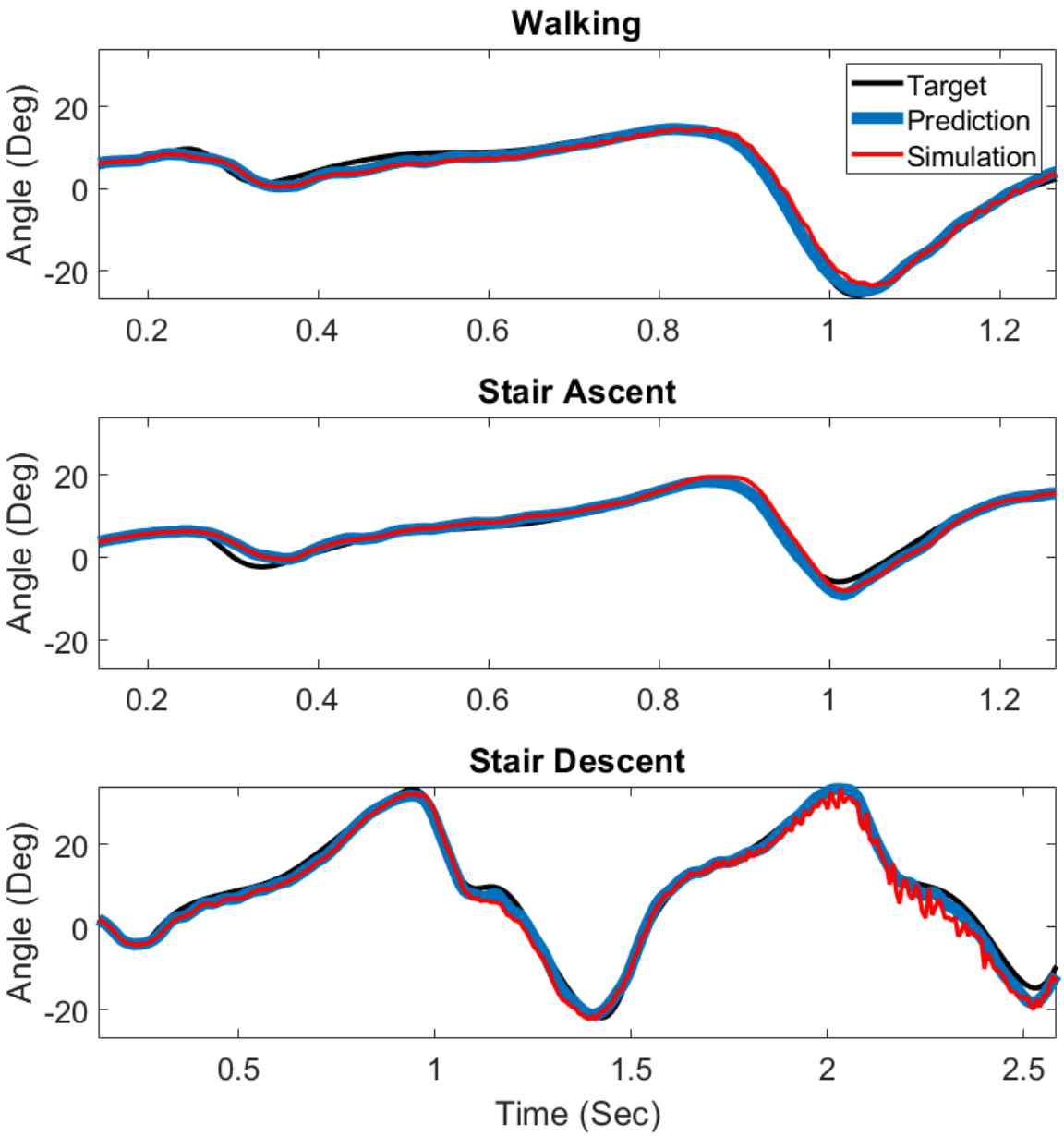

Figure 14: Average performance across task types for closed-loop control simulations with external feedback.
Each profile corresponds to the average across subjects. The average target profile is shown in black, the average NARX prediction profile is shown in blue and the average control simulation profile is shown in red. This average is not normalized.

The average absolute error tended to decrease over time during walking but approached instability toward the end of the stair descent profile in Figure 14.

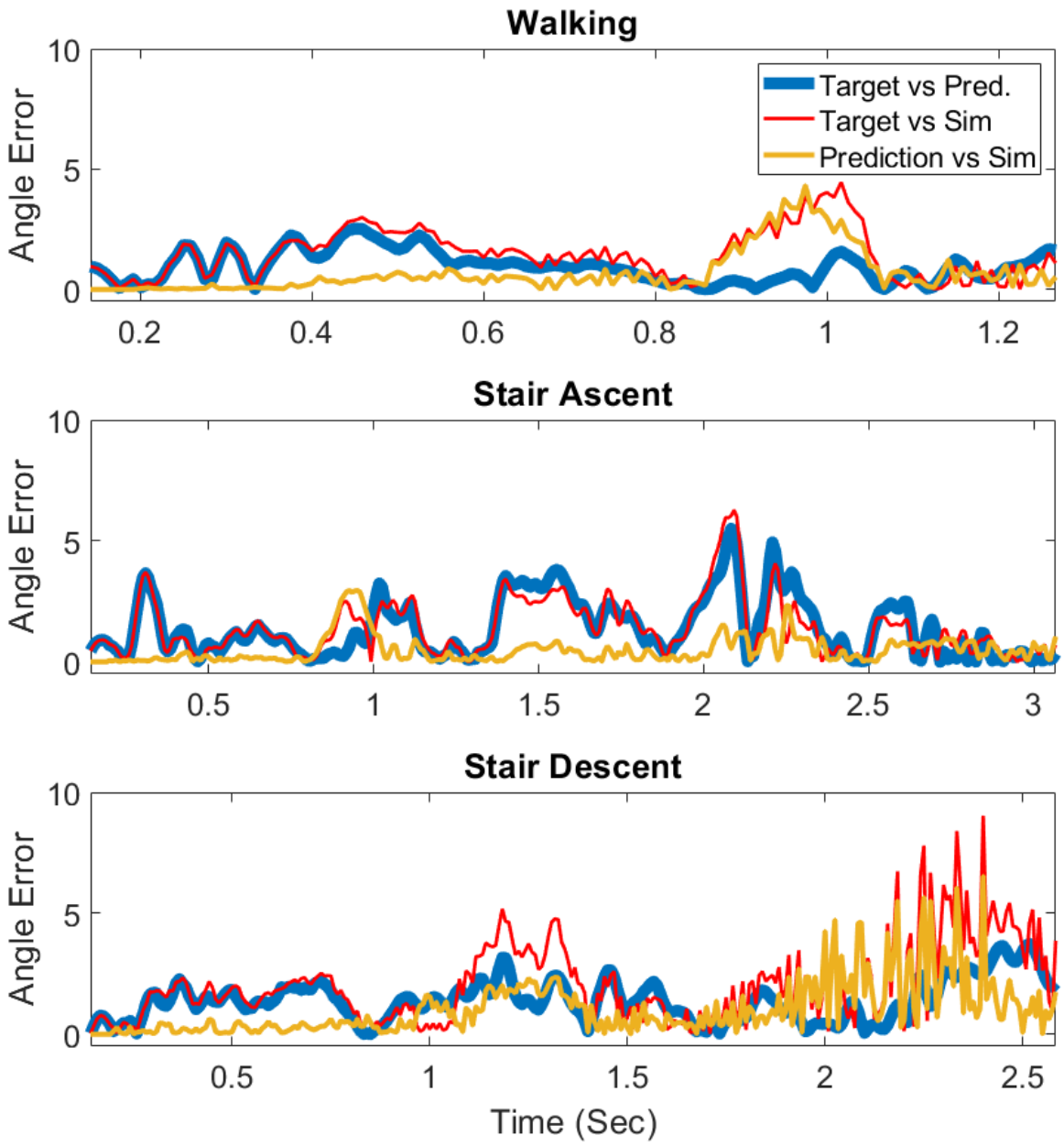

Figure 15: Average performance across task types for closed-loop control simulations with external feedback.
Each profile corresponds to the absolute error averaged across subjects. The blue line shows the error between NARX prediction and the target profile. The red line shows the error between the control simulation and the target profile, and the yellow line shows the error between the NARX prediction and control simulation output.

Figure 15 shows that even for trials that didn't fail to fully simulate, destabilization occurred over time. Destabilization was especially present for the stair descent task which also had the most failed trials for each subject.

Table 4: Difference in NARX prediction RMSE between open-loop control simulations and closed-loop control simulations with external feedback with failed trials removed. Error differences are highlighted in red. Zeros indicate a difference that does not appear on the 120 Hz timescale.

	RMSE				SD			
Subject	Walking	Ascent	Descent	Average	Walking	Ascent	Descent	Average
1	0	2.04	2.78	1.61	0	3.37	8.11	3.83
2	0	-1.93	0.81	-0.37	0	1.52	11.06	4.19
3	0	0.40	4.72	1.71	0	-12.07	12.89	0.27
4	0	3.04	-1.50	0.51	0	-24.00	10.04	-4.65
5	0	-7.53	9.89	0.78	0	1.56	-13.51	-3.98
6	0	8.81	-13.13	-1.44	0	26.76	32.02	19.59
Average	0.00	0.81	0.59	0.47	0.00	-0.47	10.10	3.21

As can be seen in Table 4, there are no failures that occurred or error detectable in the walking condition. Error increases in stair ascent and descent where the range of motion is greater. There is a great difference of error variance in the stair descent mode between subjects. The average RMSE across subjects and task types increased by 0.47 degrees.

Table 5: Difference in RMSE target vs closed-loop simulation
NARX predictions with external feedback. Comparing the target vs the simulation output with failed trials removed.

RMSE				SD			
Walking	Ascent	Descent	Average	Walking	Ascent	Descent	Average
3.10	3.04	5.12	3.75	2.15	0.64	4.13	2.31
1.51	2.90	2.82	2.41	0.20	0.65	0.29	0.38
2.02	3.30	5.09	3.47	0.71	0.99	2.97	1.56
1.90	2.58	2.50	2.33	0.44	0.28	0.44	0.39
2.19	2.58	2.99	2.59	0.40	0.75	0.65	0.60
2.31	2.47	11.71	5.50	0.62	0.50	13.54	4.89
2.17	2.81	5.04	3.34	0.75	0.64	3.67	1.69

In the full model feedback condition, there is a cross subject average error between the simulated output and the target of 3.34 ± 1.69 degrees, averaged over task types, see Table 5. Again, there is a wide range between subjects from 11.71 ± 4.89 degrees to 2.82 ± 0.38.

Table 6: Average RMSE by Subject and Task Type, Open Loop vs Closed Loop
RMSE between the open-loop NARX prediction and closed-loop control simulation with external feedback with failed trials removed.

	RMSE				SD			
Subject	Walking	Ascent	Descent	Average	Walking	Ascent	Descent	Average
1	1.33	1.48	3.45	2.09	0.66	0.84	4.46	1.99
2	0.73	1.06	1.15	0.98	0.28	0.31	0.44	0.34
3	1.28	1.77	3.80	2.28	0.88	1.24	3.56	1.89
4	1.04	0.86	0.72	0.87	0.21	0.19	0.23	0.21
5	1.30	0.96	1.10	1.12	0.29	0.19	0.37	0.28
6	0.93	0.99	11.34	4.42	0.41	0.25	15.03	5.23
Average	1.10	1.19	3.59	1.96	0.45	0.50	4.02	1.66

In the case of Table 6, the average difference among successful trials from the closed loop prediction and simulation prediction/simulation ankle output can be seen.

4. Discussion

4.0 Overview

In aim 2 it was shown that the NARX predictive model can provide desired states for a prosthesis control system. However, prior to human-in-the-loop testing, full validation will require an updated dynamic model of the prosthesis that incorporates realistic torque and ground reactions of movement.

4.1 Principles

Aside from the model adjustments made to accommodate the wider range of motion from the experimental data, incorporation of the NARX model as a control signal into the prosthesis controller simulation worked as expected. All trials for all subjects were simulated successfully across gait tasks.

The open-loop control simulation, in which the NARX model utilized internal feedback, added negligible error to the actuated ankle angle and moment. The average error between the control simulation and the NARX prediction of ankle angle was 3768 times less than the NARX prediction error averaged across ask types and subjects. With the primary source of error being resulting from the forward prediction of ankle angle and moment, further training improvement should translate into direct performance gains from the system. Across the range of network structures and parameters setting examined, the NARX model using 3 EMG + 3D velocity inputs resulted in the best overall performance across subjects for the tested types of gait (walking, stair ascent and descent). It is possible that EMG inputs from additional muscles could yield better results as suggested by (Keleş & Yucesoy, 2020) with their best predictive model including five EMG signals. More EMG inputs would yield similar computational time for the control model but would increase the amount of training required.

The original Simulink control model used a variable sample rate that was 5-10 times higher than the 120 Hz sampling used in the NARX model. To accommodate this limitation, the control simulation analysis was down sampled to 120 Hz for direct comparison to the experimental data. This difference in speed may account for the low error since the control simulation had plenty of time to adjust to changes in the NARX output. The small variations may be lost in the translation to 120 Hz but this is unlikely to be a problem since the NARX model can be trained to operate at higher sampling rates typical of EMG and physical sensor systems.

For the control simulations with external feedback of ankle angle, the model performance did not change significantly, suggesting that external feedback of ankle moment was not critical for replicating the gait profiles of ankle angle across tasks in model. By comparison, the control simulations with external feedback of both ankle angle and moment to NARX proved to be less stable due to limitations in the Simulink model. Since the moment produced by the model was not derived from the model physics of the 4-bar mechanism they had to be calculated separately. This limitation was a characteristic of the original Marquette prosthetic model, due to the lack of a full body model to replicate realistic foot loading. The inability to simulate the appropriate ankle moments in response to ground reaction forces resulted in an overall increase in the control system error with respect to the target gait profiles. Control simulation instability increased with the mismatch between the desired ankle moment generated by the NARX model and the external moment feedback obtained from the Marquette prosthetic model. Trial failures due to instability increased to 7.5 per subject with a 0% failure rate for walking trials, 33% failure rate for stair ascent trials, and a 42% failure rate for stair

descent trials on average. Across subject datasets, the number of failed trials in the stair ascent condition ranged from 10% to 60% and ranged from 20% to 80% in the stair descent condition. Among successful trials, the average angle RMSE increased by 1.96 ± 1.66 degrees relative to the NARX prediction.

Based on the control simulation performance with external feedback of ankle angle, it is expected that stability would improve if the prosthetic model replicated the realistic moment response during gait. There was zero measurable error recorded from adding external angle feedback so it is expected that the inclusion of accurate external moment feedback would result in lower overall controller error. Until a model with accurate moment feedback is incorporated, it is difficult to determine the extent of the error tolerance for the predictive system. One way error produced by the system could be simulated would be by adding random noise to NARX model feedback. Finally, the range of experimentally measured ankle angles suggests that the mechanical structure of the Marquette prosthetic system may need to be modified to achieve a wider range of gait profiles across users. In other words, the range of motion possible in the model was insufficient to simulate the range of motion of the data set used in this thesis and that could bear out in the real hardware.

4.2 Exceptions

The gait profiles for one subject proved particularly problematic for the original system, and ultimately required that the length of the L3 bar be doubled. Limitations to the range of motion were most prominent for stair descent trials. The maximum angles of the target profiles were all close to or exceeded the maximum allowed angle of the adjusted

4-bar mechanism. For this subject, a further adjustment to 4.3 cm was necessary to successfully run the control simulation across trials.

Further adjustments to the prosthesis may be warranted depending on the range of mobility desired. The adjustment in this study did not have a noticeable impact on the capability to accurately drive simulated ankle actuation. However, further adjustments to the mechanism's dimensions will have an impact on the amount of motor torque required. Additionally, although motor simulation occurs another layer of reality that is lacking is the motor actuation time. In the physical implementation of the control system, the NARX prediction ahead of time will be used to counteract lag but this effect on error or instability would still need to be studied.

In the case of the external angle and moment feedback model, the adjustment made to the prosthetic model was not sufficient to successfully simulate all trials. The failures typically occurred where error built up until the control system became unstable, with enough error the simulations maximum RoM was violated and the simulation ended prematurely. The main way to rectify this problem would be more accurately simulating the moment feedback of the prosthesis during gait. Again, it is possible this issue would not be present in the real-world system when moment would be applied realistically.

4.3 Previously Published works

Importantly, current systems are generally lacking in their ability to provide smooth gait transitions and their ability to account for lag in the control and motor actuation. Continuous control for lower limb prosthetic devices is still a novel and growing field of development. As discussed previously, predictive ankle models are

another developing area and continuous predictive prosthesis control remains underdeveloped.

The vast majority of powered transtibial prosthesis control systems can be classified as finite state machines. They break gait down into a continuous repetition of phases (Sun et al., 2014). Many of these systems have attempted to incorporate multiple mobility tasks (Kannape & Herr, 2014) (Culver et al., 2018) to varying degrees of success. Task switching and volitional control are two methods used to account for changes in gait, such as when transitioning from level ground walking to stair ascent.

Among finite state control models, one of the most well developed on is BioM, developed by Dr. Hugh Herr and studied at MIT. The controller for the BioM was originally intended for walking conditions only (Wang et al., 2013). Operating in this mode did not give the user the power input required to properly ascend stairs. Tests were performed to adapt the device to accommodate stair ascent using volitional control (Kannape & Herr, 2014). In the volitional control model, a proportional EMG signal was used to modulate the ankle extension and power desire for stair ascent. However, the appropriate controlled powered output was not achieved. In a more recent study by (Culver et al., 2018), the finite state model did not incorporate proportional EMG control and was shown to provide improved torque characteristics in stair ascent and stair descent cases compared to a passive prosthesis.

As stated in the purpose for this study, a continuous model circumvents the challenges of increasing the complexity of a finite state system to meet the varied needs of a user. In that regard, the ability to accurately predict and provide control outputs for multiple mobility tasks and task transitions have been demonstrated to work in a

simulation of a real prosthetic device. This continuous approach may be computationally simpler than incorporating new finite states and transitions to account for all gait scenarios.

In regard to human-in-the-loop (HIL) training, it's hard to compare this study because the subject data being used was quasi-static. In a human-in-the-loop simulation, the subject is considered part of the control system rather than an external input to the system. Further exploration of the effect of HIL control would require subject testing.

4.4 Practical Implications

The implications of lagless continuous control extend beyond use in transtibial prostheses. The approach is applicable to other types of prosthetic devices such as transfemoral prostheses or upper extremity prosthesis. In power exoskeletons or other EMG based control systems, predictive control improves usability by eliminating system lag.

Across applications, implementing a predictive NARX model for EMG-based control requires the collection of training data sampled at rates appropriate to the control system. It's still unknown how the predictive system would respond to human-in-the-loop changes in EMG and movement kinetics/kinematics or whether the control system itself may lead to subject specific changes in EMG patterns over time to improve controllability.

4.5 Main Take Away and Significance Towards Future Works

The internal feedback NARX model functioned as desired with little to no error. External model feedback to the NARX model may work in the future considering the success of external angle feedback but does not work with the current ankle moment

approximation of the model. As it stands the lag-compensated and continuous nature of the model is could be promising for lower limb prosthesis where a delay in actuation can create major falling hazards, again, real world testing will need to be done to prove this.

Future studies might include employing a prosthesis simulation that incorporates a full body model to better simulate moment mechanics. It would also be important to evaluate the error tolerance of the NARX external feedback model as it has been shown in the failed simulation trials that certain levels of error can lead to destabilization. In addition to more sophisticated model testing, real world testing on the prosthetic device could also be used to provide appropriate moment feedback. Real world testing, however, might prove challenging because the measurement of EMG signals within socket and velocity signals from the prosthesis would need to be integrated into the physical system design. Preliminary testing on real world subjects would need to be done using a harness system to prevent falling in case of prosthesis instability.

This study used data from six subjects. It is possible a larger study utilizing more subject data could lead to a predictive model that is generalizable across subjects. This type of model would not require individual training, but it seems unlikely that a subject independent model would achieve the low RMSE obtained with subject specific NARX models. What might prove interesting to study is a set of data that includes less rigid and therefore more varied data. Such tasks could include ramp ascent and descent which incorporates variable foot placement. Acquiring more free form trials with the current experimental setup would be difficult to achieve due to limitations in the size of the motion capture space and the need for multi-axis measurements of ground reaction force to characterize ankle moment during gait.

Another possibility would be to create a generalized NARX model. Such a model could provide a generic prosthesis control but would prove to be less ideal that one individual attune to the user. However, if similarities in the EMG profiles of amputees were theoretically found, a general model could provide the basis for an adaptive control model for prosthetic use. That is, one that starts from some baseline function and then adapts to the user's profile through use.

Finally, it is likely that other predictive network models could work just as well as the NARX model. It was found the model needed to be nonlinear and does need external inputs but other networks that fit that criteria could work.

IV. CONCLUSION

1. Findings

This study examined the use of predictive networks for closed-loop control of ankle angle and moment for use in a transtibial prosthesis. The capability of the system to be quickly optimized for the individual user and the ability to operate in real time without conscious input from the user, could improve prosthesis control when coupled with robust prediction across different types of ambulation.

In the thesis, results demonstrate that a closed-loop nonlinear autoregressive network can be trained to accurately predict ankle angle and moment from kinetic, kinematic, and myoelectric inputs across level ground walking, stair ascent, and stair descent tasks. Six input E+V networks used the combination of 3D ankle shank velocity and 3 EMG signals to predict ankle angle and moment across multiple mobility tasks with an average angle RMSE of 2.37 degrees and average moment RMSE of 0.0837 N*m/kg. The best-found networks used 16 nodes and predicted 58.33 ms ahead of time with a 120 ms sample window. This result is enough to account for system lag and facilitate instantaneous control of a prosthetic device.

In Aim 2, computer model simulation of prosthesis control using the network in real time using static EMG and ankle velocity signals matched with average RMSE 7.39E-04 degree versus target timeseries. Using feedback from the simulated ankle angle proved as successful but the use of imperfect moment calculation as feedback to the NARX network produced error build. A model that incorporates proper subject weight and GRF is necessary to properly test that type of feedback.

2. Implications

Continuous predictive control across mobility tasks helps to circumvent the dilemma of an ever-expanding finite state model. Instead of incorporating more states or more volitional control, one must only fine tune their training data sets to improve performance or include new forms of movement. It's possible that there is some limit to this exact type of method, during the process of picking the appropriate networks, some error was still present, if not less so than some of the other studies analyzed in this paper. Still, molding data sets is far simpler than designing a finite state model to react to every new situation.

As for the predictive nature of the control, the implication of lagless control is also very helpful for overcoming input lag of a prosthetic device and the user's perceived fluidity of control. This type of lag is a constant and unavoidable issue in traditional proportional control. However, the type of lag generated by a user's change in movement intent, such as changing directions on a whim will obviously still generate some lag in the response of predictive control due to the averaging of previous data points. Although there is no way around this type of lag, it is still a possible problem is end-user control that should be explored.

The finding that networks of this nature perform best with a relatively small (16 node) architecture also aids in real life implementation. The fewer nodes in the network, the fewer computations occur at each sample interval and the faster the network can be trained. Compared to some of the methods discussed in other papers, these networks seem to do well even against more complicated network structures. The main takeaway from this benefit is an aid in the iterative process of developing low error networks. More networks can be trained faster in different permutations. Furthermore, for the

deployment of commercial machine trained prosthetic devices, fast and relatively resource non-intensive computer training could be used to implement practical and painless recalibration to the available options of prosthetists or even end users for affordable means of customization.

Implications of the types of inputs found to be effective are a limit to the number of necessary sensors needed to run such a network. The more sensors needed, the greater cost and complexity of design. Using sEMG with onboard accelerometry is all that is needed for this type of network. No need for complicated integration of feedback from the prosthesis itself. This method still requires the implementation of a prosthesis socket that incorporates the sensors in a way that maintains user comfort and consistent sensor contact so limiting the number of needed sensors is important. It is likely that even simpler methods could be achieved with the use of thin sEMGs unintrusively layered inside the prosthesis's socket and accelerometers mounted on the outside surface of the prosthesis itself making modification of the prosthesis socket limited or unnecessary.

3. Future Directions

Further testing for amputee data would be necessary to gage the effect of using residual muscle signals. Strategies such as using different combinations of muscles to account for non-standard residual muscle EMG behavior or other post amputation variables may be necessary. It would also stand to reason that the adaptation/degradation amputee user muscles experience over time would change the ability for the network to predict movement properly. A long-term study may be needed as changes in muscle activity over time is far more likely in the amputee population which the technology was originally intended for.

In addition, further forms of movement may be helpful to include in network training data sets. Data such as walking up and down ramps can provide a more heterogeneous set of data and may add further robustness to predictions. Furthermore, data including different types of movement starting and stopping patterns, such as gradual or abrupt stops could help round out functions of the network prediction. Though as of now it is not clear how networks of these types will react to other forms of data. The last main important sets of data that should be used for testing these networks is real time data. In Aim 2 the feasibility of trained networks was tested against static data. Human-in-the-loop testing is an important factor. The device will react to user input, but the feedback does not stop there in a real system. All these factors would seem necessary to take this technology to the next level.

Applications of this lagless continuous control should be possible for different types of prosthetic devices or in myoelectrically controlled exoskeletons for rehabilitation or industrial means. User control of such devices in a natural and intuitive way leveraging their own muscle movements could improve these technologies greatly.

BIBLIOGRAPHY

Au, S., Berniker, M., & Herr, H. (2008). Powered ankle-foot prosthesis to assist level-ground and stair-descent gaits. *Neural Networks*, *21*(4). https://doi.org/10.1016/j.neunet.2008.03.006

Braun, S. (2001). SIGNAL PROCESSING, MODEL BASED METHOD. *Encyclopedia of Vibration*, 1199–1208. https://doi.org/10.1006/RWVB.2001.0054

Choi, J. T., & Bastian, A. J. (2007). Adaptation reveals independent control networks for human walking. *Nature Neuroscience*, *10*(8). https://doi.org/10.1038/nn1930

Culver, S., Bartlett, H., Shultz, A., & Goldfarb, M. (2018). A Stair Ascent and Descent Controller for a Powered Ankle Prosthesis. *IEEE Transactions on Neural Systems and Rehabilitation Engineering : A Publication of the IEEE Engineering in Medicine and Biology Society*, *26*(5), 993–1002. https://doi.org/10.1109/TNSRE.2018.2819508

Dey, S., Eslamy, M., Yoshida, T., Ernst, M., Schmalz, T., & Schilling, A. (2019). A support vector regression approach for continuous prediction of ankle angle and moment during walking: An implication for developing a control strategy for active ankle prostheses. *IEEE International Conference on Rehabilitation Robotics*, *2019-June*. https://doi.org/10.1109/ICORR.2019.8779445

Eslamy, M., & Alipour, K. (2018). Synergy-Based Gaussian Process Estimation of Ankle Angle and Torque: Conceptualization for High Level Controlling of Active Robotic Foot Prostheses/Orthoses. *Journal of Biomechanical Engineering*, *141*(2). https://doi.org/10.1115/1.4041767

Farmer, S., Silver-Thorn, B., Voglewede, P., & Beardsley, S. A. (2014). Within-socket myoelectric prediction of continuous ankle kinematics for control of a powered transtibial prosthesis. *Journal of Neural Engineering*, *11*(5), 1–20. https://doi.org/10.1088/1741-2560/11/5/056027

Gardiner, J., Bari, A. Z., Howard, D., & Kenney, L. (2016). Transtibial amputee gait efficiency: Energy storage and return versus solid ankle cushioned heel prosthetic feet. *Journal of Rehabilitation Research and Development*, *53*(6), 1133–1138. https://doi.org/10.1682/JRRD.2015.04.0066

Gehlhar, R., Tucker, M., Young, A. J., & Ames, A. D. (2023). A review of current state-of-the-art control methods for lower-limb powered prostheses. *Annual Reviews in Control*, *55*, 142–164. https://doi.org/10.1016/J.ARCONTROL.2023.03.003

Grimmer, M., Holgate, M., Holgate, R., Boehler, A., Ward, J., Hollander, K., Sugar, T., & Seyfarth, A. (2016). A powered prosthetic ankle joint for walking and running. *BioMedical Engineering OnLine*, *15*(Suppl 3). https://doi.org/10.1186/S12938-016-0286-7

Gupta, R., Dhindsa, I. S., & Agarwal, R. (2020). Continuous angular position estimation of human ankle during unconstrained locomotion. *Biomedical Signal Processing and Control*, *60*. https://doi.org/10.1016/j.bspc.2020.101968

Hansen, J, M., A, P., & J., H. (2016). *Prosthetic Feet Fact Sheet*. 1–3. http://www.amputee-coalition.org/resources/prosthetic-feet/

Hoover, C. D., Fulk, G. D., & Fite, K. B. (2013). Stair ascent with a powered transfemoral prosthesis under direct myoelectric control. *IEEE/ASME Transactions on Mechatronics*, *18*(3). https://doi.org/10.1109/TMECH.2012.2200498

Huang, H., Kuiken, T. A., & Lipschutz, R. D. (2009). A strategy for identifying locomotion modes using surface electromyography. *IEEE Transactions on Biomedical Engineering*, *56*(1). https://doi.org/10.1109/TBME.2008.2003293

Huang, S., Wensman, J. P., & Ferris, D. P. (2016). Locomotor Adaptation by Transtibial Amputees Walking with an Experimental Powered Prosthesis under Continuous Myoelectric Control. *IEEE Transactions on Neural Systems and Rehabilitation Engineering*, *24*(5). https://doi.org/10.1109/TNSRE.2015.2441061

Huihui, C., Farong, G., Chao, C., & Taixing, T. (2018). Estimation of ankle angle based

on multi-feature fusion with random forest. *Chinese Control Conference, CCC, 2018-July*. https://doi.org/10.23919/ChiCC.2018.8482982

Kannape, O. A., & Herr, H. M. (2014). Volitional control of ankle plantar flexion in a powered transtibial prosthesis during stair-ambulation. *2014 36th Annual International Conference of the IEEE Engineering in Medicine and Biology Society, EMBC 2014*, 1662–1665. https://doi.org/10.1109/EMBC.2014.6943925

Kannape, O. A., & Herr, H. M. (2016). Split-belt adaptation and gait symmetry in transtibial amputees walking with a hybrid EMG controlled ankle-foot prosthesis. *Annual International Conference of the IEEE Engineering in Medicine and Biology Society. IEEE Engineering in Medicine and Biology Society. Annual International Conference*, *2016*, 5469–5472. https://doi.org/10.1109/EMBC.2016.7591964

Keleş, A. D., & Yucesoy, C. A. (2020). Development of a neural network based control algorithm for powered ankle prosthesis. *Journal of Biomechanics*, *113*. https://doi.org/10.1016/j.jbiomech.2020.110087

Klein, J. (2018). *Control Design and Implementation of an Active Transtibial Prosthesis*. *2*, 41–43.

Kuiken, T. A., Li, G., Lock, B. A., Lipschutz, R. D., Miller, L. A., Stubblefield, K. A., & Englehart, K. B. (2009). Targeted muscle reinnervation for real-time myoelectric control of multifunction artificial arms. *JAMA - Journal of the American Medical Association*, *301*(6), 619–628. https://doi.org/10.1001/jama.2009.116

Loverro, K. L., Mueske, N. M., & Hamel, K. A. (2013). Location of minimum foot clearance on the shoe and with respect to the obstacle changes with locomotor task. *Journal of Biomechanics*, *46*(11). https://doi.org/10.1016/j.jbiomech.2013.05.002

Pearson, K. G. (2000). Neural adaptation in the generation of rhythmic behavior. In *Annual Review of Physiology* (Vol. 62). https://doi.org/10.1146/annurev.physiol.62.1.723

Prasertsakul, T., Poonsiri, J., & Charoensuk, W. (2012). Prediction gait during ascending

stair by using Artificial Neural Networks. *5th 2012 Biomedical Engineering International Conference, BMEiCON 2012*. https://doi.org/10.1109/BMEiCon.2012.6465464

Protopapadaki, A., Drechsler, W. I., Cramp, M. C., Coutts, F. J., & Scott, O. M. (2007). Hip, knee, ankle kinematics and kinetics during stair ascent and descent in healthy young individuals. *Clinical Biomechanics*, *22*(2). https://doi.org/10.1016/j.clinbiomech.2006.09.010

Silver-Thorn, B., Current, T., & Kuhse, B. (2012). Preliminary investigation of residual limb plantarflexion and dorsiflexion muscle activity during treadmill walking for trans-tibial amputees. *Prosthetics and Orthotics International*, *36*(4). https://doi.org/10.1177/0309364612443379

Sinitski, E., Baddour, N., Gholizadeh, H., Besemann, M., Dudek, N., & Lemaire, E. (2022). Cross slope gait biomechanics for individuals with and without a unilateral transtibial amputation ☆. *Clinical Biomechanics*, *98*, 105734. https://doi.org/10.1016/j.clinbiomech.2022.105734

Sinitski, E. H., Hansen, A. H., & Wilken, J. M. (2012). Biomechanics of the ankle-foot system during stair ambulation: Implications for design of advanced ankle-foot prostheses. *Journal of Biomechanics*, *45*(3). https://doi.org/10.1016/j.jbiomech.2011.11.007

Siu, H. C., Sloboda, J., McKindles, R. J., & Stirling, L. A. (2021). A Neural Network Estimation of Ankle Torques From Electromyography and Accelerometry. *IEEE Transactions on Neural Systems and Rehabilitation Engineering : A Publication of the IEEE Engineering in Medicine and Biology Society*, *29*, 1624–1633. https://doi.org/10.1109/TNSRE.2021.3104761

Smith, L. H., Hargrove, L. J., Lock, B. A., & Kuiken, T. A. (2011). Determining the optimal window length for pattern recognition-based myoelectric control: Balancing the competing effects of classification error and controller delay. *IEEE Transactions on Neural Systems and Rehabilitation Engineering*, *19*(2), 186–192.

https://doi.org/10.1109/TNSRE.2010.2100828

Su, B. Y., Wang, J., Liu, S. Q., Sheng, M., Jiang, J., & Xiang, K. (2019). A cnn-based method for intent recognition using inertial measurement units and intelligent lower limb prosthesis. *IEEE Transactions on Neural Systems and Rehabilitation Engineering*, *27*(5), 1032–1042. https://doi.org/10.1109/TNSRE.2019.2909585

Su, P. F., Gard, S. A., Lipschutz, R. D., & Kuiken, T. A. (2008). Differences in Gait Characteristics Between Persons With Bilateral Transtibial Amputations, Due to Peripheral Vascular Disease and Trauma, and Able-Bodied Ambulators. *Archives of Physical Medicine and Rehabilitation*, *89*(7), 1386–1394. https://doi.org/10.1016/j.apmr.2007.10.050

Sun, J., Fritz, J. M., Del Toro, D. R., & Voglewede, P. A. (2014). Amputee subject testing protocol, results, and analysis of a powered transtibial prosthetic device. *Journal of Medical Devices, Transactions of the ASME*, *8*(4), 1–6. https://doi.org/10.1115/1.4027497

Wang, J., Kannape, O. A., & Herr, H. M. (2013). Proportional EMG control of ankle plantar flexion in a powered transtibial prosthesis. *IEEE International Conference on Rehabilitation Robotics*. https://doi.org/10.1109/ICORR.2013.6650391

Winter, D. A. (2009). Biomechanics and Motor Control of Human Movement: Fourth Edition. *Biomechanics and Motor Control of Human Movement: Fourth Edition*, 1–370. https://doi.org/10.1002/9780470549148

Young, A. J., Kuiken, T. A., & Hargrove, L. J. (2014). Analysis of using EMG and mechanical sensors to enhance intent recognition in powered lower limb prostheses. *Journal of Neural Engineering*, *11*(5). https://doi.org/10.1088/1741-2560/11/5/056021

Zabre-Gonzalez, E. V., Riem, L., Voglewede, P. A., Silver-Thorn, B., Koehler-McNicholas, S. R., & Beardsley, S. A. (2021). Continuous Myoelectric Prediction of Future Ankle Angle and Moment Across Ambulation Conditions and Their

Transitions. *Frontiers in Neuroscience*, *15*. https://doi.org/10.3389/FNINS.2021.709422

Zarshenas, H., Ruddy, B. P., Kempa-Liehr, A. W., & Besier, T. F. (2020). Ankle torque forecasting using time-delayed neural networks. *Proceedings of the Annual International Conference of the IEEE Engineering in Medicine and Biology Society, EMBS*, *2020-July*, 4854–4857. https://doi.org/10.1109/EMBC44109.2020.9175376

APPENDIX AIM 1

Statistics for Network Methods

EMG	Angle		RMSE/ROM %		Moment		RMSE/ROM %	
	Avg	Std	%	Std	Avg	STD	%	Std
Walking	4.10	0.85	11.60	2.41	0.12	0.04	7.30	2.12
Up	4.89	0.67	9.72	1.33	0.17	0.02	10.63	1.54
Down	5.75	1.76	9.41	2.89	0.17	0.05	11.18	2.97
All	4.92	1.37	10.24	2.86	0.15	0.04	9.70	2.73

VEL	Angle		RMSE/ROM %		Moment		RMSE/ROM %	
	Avg	Std	%	Std	Avg	STD	%	Std
Walking	2.22	0.36	6.21	1.01	0.10	0.02	5.94	1.15
Up	3.20	0.66	6.32	1.30	0.14	0.03	8.69	2.04
Down	3.37	0.29	5.52	0.47	0.13	0.02	8.33	1.39
All	2.93	0.69	6.02	1.41	0.12	0.03	7.65	1.90

E+V	Angle		RMSE/ROM %		Moment		RMSE/ROM %	
	Avg	Std	%	Std	Avg	STD	%	Std
Walking	1.87	0.36	5.27	1.00	0.06	0.02	3.60	1.02
Up	2.62	0.51	5.21	1.01	0.09	0.02	5.63	1.00
Down	2.61	0.49	4.28	0.80	0.10	0.02	6.61	1.31
All	2.37	0.57	4.92	1.19	0.08	0.03	5.28	1.60

Table 7: (Appendix) Average RMSE and RMSE/ROM across networks
Looking at the first box: EMG. In rows, you have the average statistic of the column for the walking condition (Walking), stair ascent condition (Up), stair descent condition (Down), and overall average (All). In the first four column, there are the average RMSE in angle predictions, average standard deviation in angle, the average percentage of RMSE/ROM in angle predictions, the average percentage of standard deviation of RMSE/ROM in angle predictions. In the second four columns, there are the same statistics for the moment predictions. This format is the same for each set EMG, VEL, E+V.

In Table 7 RMSE is averaged across each entire time course and the average RMSE in each condition is the average of each RMSE over time. For angle predictions,

level ground walking prediction always the best, followed by stair ascent, and then stair descent for EMG and VEL network. For E+V networks the stair ascent and stair descent averages differ by only 0.01 degrees within the standard deviation. For moment predictions, level ground walking is still best but again there is no clear winner between stair ascent and descent differing between 0 to 0.01 within the standard deviation. The statistic RMSE/ROM represents the ratio of the average RMSE to the average ROM, range of motion, shown in the table as a percentage. This statistic represents a unitless interpretation of what the RMSE means compared to the entire movement. In other words, if a trials range of motion is low an equivalent RMSE would represent a larger percentage than for a trial with a higher range of motion. If one considers a lower range of motion movement to have a lower tolerance for error, RMSE/ROM may hold a useful comparison. On the other hand, a movement with a larger range of motion will end up having a larger variability in input and therefore a larger variability in average outputs and in output error.

Table 8: (Appendix) Average Correlation Coefficient
Shown is the average correlation coefficient for each of the three network types. In rows, each mobility condition and in each column corresponding to angle and moment for EMG networks, then for velocity networks, then E+V networks.

	EMG		Vel		E+V	
	q	t	q	t	q	t
Walking	0.88404	0.97578	0.96777	0.98834	0.97517	0.99429
Up	0.91517	0.93631	0.96577	0.9565	0.97765	0.98182
Down	0.92962	0.93736	0.97892	0.96781	0.98798	0.97832
Average	0.90961	0.949817	0.97082	0.970883	0.980267	0.98481

Table 9: (Appendix) Percent increase in correlation of moment over angle
Shown is the percentages of moment correlation compared to angle correlation, (t/q-1) * 100%. A positive percentage indicated greater performance in moment prediction and a negative indicated a greater performance in angle prediction.

	EMG	Vel	E+V	Avg
Walking	10.37736	2.125505	1.960684	4.821182
Up	2.309953	-0.95986	0.426533	0.59221
Down	0.832598	-1.13492	-0.97775	-0.42669
Average	4.420209	0.006524	0.463479	1.630071

As can be seen in Table 11, the largest disparity in training occurred in the walking condition for EMG network, 10.4%. For each network, the bias towards moment performance is highest in the walking condition. In the velocity and E+V networks cases, there was a small or even negative bias. The average bias is greatest in the EMG networks case, almost zero in the velocity networks case, and very small in the E+V networks case (10x less than the EMG network).